Acoustic Environment of Haro Strait: Preliminary Propagation Modeling and Data Analysis

by Christopher D. Jones and Michael A. Wolfson

Applied Physics Laboratory   University of Washington
1013 NE 40th Street   Seattle, Washington 98105-6698

Acknowledgments

Abstract

Field measurements and acoustic propagation modeling for the frequency range 1–10 kHz are combined to analyze the acoustic environment of Haro Strait of Puget Sound, an area frequented by the southern resident killer whales. Haro Strait is a highly variable acoustic environment with active commercial shipping, whale watching, and Naval activity. Southern resident killer whales are of unique public concern in this area because of increasing anthropogenic noise levels that may interfere with the animal's foraging strategies and behavior. Predictive acoustic modeling in combination with field measurements can be used as a tool for understanding the mechanisms of impact and assessment of the risk, providing a quantitative evaluation of sound source levels in the context of complicated acoustic environments, changing background sound levels, and emerging management issues. Of principle concern here is background sound levels created by commercial shipping traffic or other persistent sound sources that propagate from the main shipping channel. The scope of the modeling effort encompasses numerical modeling of transmission loss and propagation at ranges of less than 10 km. Preliminary modeling results are analyzed and compared with recordings of ship noise collected in the spring/summer of 2004.

Contents

1.   Introduction

Haro Strait is a complex, shallow water acoustic environment with steep bathymetric relief combined with an active shipping channel, frequent small boat activity, and Naval operations. The western side of San Juan Island is also a primary foraging area for the southern resident killer whales.[1] These animals are of unique public concern in this area because of the potentially high impact of human activity on their environment. Questions regarding the acoustic environment of these animals have arisen as recreational whale watching, commercial shipping, and Naval activity[2] have grown in this area. Are increasing underwater noise levels affecting the killer whales' ability to forage for prey by echo-location? Studies of the echo-location signals from killer whales[3] indicate that backscattered signal levels from salmon can be very low and comparable in level to natural background noise levels.

This report addresses specific aspects of modeling the propagation of sound sources in Haro Strait, focusing on the numerical estimation of transmission loss in the open channel. In particular, we investigated the propagation of sound generated by large commercial ship traffic in the strait and the estimation of sound source levels of individual ships. We illustrate the role of modeling as a tool for model/data comparisons and the interpretation of field measurements of underwater sound. In this process we employed a variety of compiled databases of the environment, information on ship traffic and vessel tracking, and field measurements of underwater noise collected recently in Haro Strait in an area frequented by killer whales.

Here, acoustic modeling is used to complement field measurements, as the shallow water environment of Haro Strait is far too complex, and the geo-acoustic parameters of the area are not characterized well enough to rely on modeling alone. When modeling is constrained by measurements it can provide a useful tool to fill the gaps in measurements in both space and time. For example, measured data are shown for a specific receiver location and time, and modeling results are compared to this data to infer source levels of

---

[1] Bigg, M.A., P.F. Olesiuk, G.M. Ellis, J.K.B. Ford, and K.C. Balcomb III, 1990. "Social organization and genealogy of resident killer whales (*orcinus orca*) in the coastal waters of British Columbia and Washington State," In: Hammmond, P.S., S.A. Mizroch, and G.P. Donovan (eds.), *Use of Photo-identification and Other Techniques to Estimate Population Parameters*. Report of the International Whaling Commission, Special Issue 12, pp. 386–406.

[2] National Marine Fisheries Service, 2005, *Assessment of Acoustic Exposures on Marine Mammals in Conjunction with USS* Shoup *Active Sonar Transmissions in the Eastern Strait of Juan de Fuca and Haro Strait, Washington, 5 May 2003*, National Marine Fisheries Service, Office of Protected Resources, January 21, 2005.

[3] Au, W.W.L., J.K.B. Ford, J.K. Horne, and K.A. Newman-Allman, 2004. "Echolocation signals of free-ranging killer whales (*Orcinus orca*) and modeling of foraging for Chinook salmon (*Oncorhynchus tshawytscha*)," *J. Acoust. Soc. Am.*, 56, 1280–1290.

individual large commercial ships. If model results compare favorably and confidence is developed in the modeling strategy for this particular area, then the model may be used to estimate sound pressure levels at other locations in the region where measurements are not available.

1.1.   Objectives and scope

The objective of this study is to determine the feasibility of modeling the sound propagation environment of the southern resident killer whales in Haro Strait and to compare initial model results with acoustic measurements taken in June and July 2004. Model/data analysis is limited to data provided by Jeff Nystuen (APL-UW) recorded on the PAL system. A significant portion of this effort involves collecting and compiling a database of environmental parameters required for acoustic modeling. The longer-term objectives are to extend these methodologies for model/data analysis by incorporating new acoustic data, more detailed environmental data, and new information on sound sources (e.g., shipping data) as they become available.

The scope of the modeling effort encompasses propagation modeling using readily available methods and codes[4] and the interpretation of existing acoustic data sets. Modeling and data analysis are focused at the frequency of 3.6 kHz, which is representative of the 1–10-kHz frequency range (within killer whale auditory response). The modeling can be extended to lower frequencies. However, extending the models to higher frequencies (>10 kHz) is problematic due to the sensitivity of the model to uncertainties in the geo-acoustic environment at high spatial scales. Modeling high-frequency propagation (>10 kHz) and reverberation is beyond the scope of this study.

The area of interest is limited to Haro Strait with propagation ranges less than 10 km. However, the methods can be applied to larger scale studies such as in the coastal ocean or different regions (e.g., beaked whale habitat). We will investigate the effects of canyons and steep walls on forward propagation combined with randomness in the sea surface and the seafloor. We will include the effects of temporal and spatial variability in the environment to model and gain insight on how sound propagation may change as a function of time and location.

1.2.   Technical approach

Here, the acoustic environment is characterized by *propagation loss* only. Defined in terms of the standard sonar equation,[5] propagation loss is the amount of signal intensity

---

[4] Ocean Acoustic Library at www.hlsresearch.com/oalib/
[5] Medwin, H., and C.S. Clay, 1998. *Acoustical Oceanography*, Academic Press.

lost as it propagates from a source to a receiver location. The numerical simulations will provide an estimate of the mean propagation loss between two positions and the variability of the estimate as a function of randomness and uncertainty in the environment. Both the mean and the associated variability (uncertainty bounds) of the estimate are necessary to compare simulation results with field measurements.

In general, propagation between two locations in the ocean includes both the direct propagation path between a source and a receiver and reverberation. Reverberation is the reflection and scattering of an acoustic signal as a result of its interaction with inhomogeneities and boundaries in the ocean. Here acoustic propagation modeling is performed using two-dimensional parabolic equation (PE) numerical methods.[6] This type of propagation modeling includes only that component of reverberation in the forward direction, such as forward scattering from the sea surface and bottom. No backscattering is included (echoes back from a canyon wall, for example).

The application of PE simulations, as typically used in lower frequency, open-ocean modeling, requires special attention when used in shallow water environments. Improper application will likely produce results that will be difficult to compare with field measurements. Modeling issues that are given special attention include:
1) Effects of random roughness at the sea surface and sea bottom that impact propagation at the frequencies of interest in this study.
2) Analysis of acoustic variability due to such randomness and the definition of uncertainty bounds for the model predictions.
3) High spatial resolution characterization of the geo-acoustic parameters (i.e., sediment properties, high-resolution bathymetry, sound speed profiles).

---

[6] Jensen, F.B., W.A. Kuperman, M.B. Porter, and H. Schmidt, 2000. *Computational Ocean Acoustics*, Springer-Verlag.

2.   Environmental Characterization

2.1.   Bathymetry

The bathymetry of Haro Strait is characterized by a relatively deep canyon with a very steep wall at the western coast of San Juan Island. The channel rises to a relatively shallow region to its west (Figures 2.1 and 2.2). Because bathymetry is a critical component of understanding acoustic propagation, a high-resolution bathymetry database of Haro Strait has been compiled with data from several sources. The highest resolution bathymetry (to our knowledge) is a recent multi-beam survey conducted by Monterey Bay Marine Laboratory (G. Greene, personal communication, 2004) providing partial coverage of the area of interest with a 5-m grid spacing. The other primary sources of lower resolution bathymetric data are NOAA and USGS.[7] These data where combined to provide a continuous bathymetric grid of the region at grid scales up to 5 m. In practice, 20-m grid spacing was adequate for modeling.
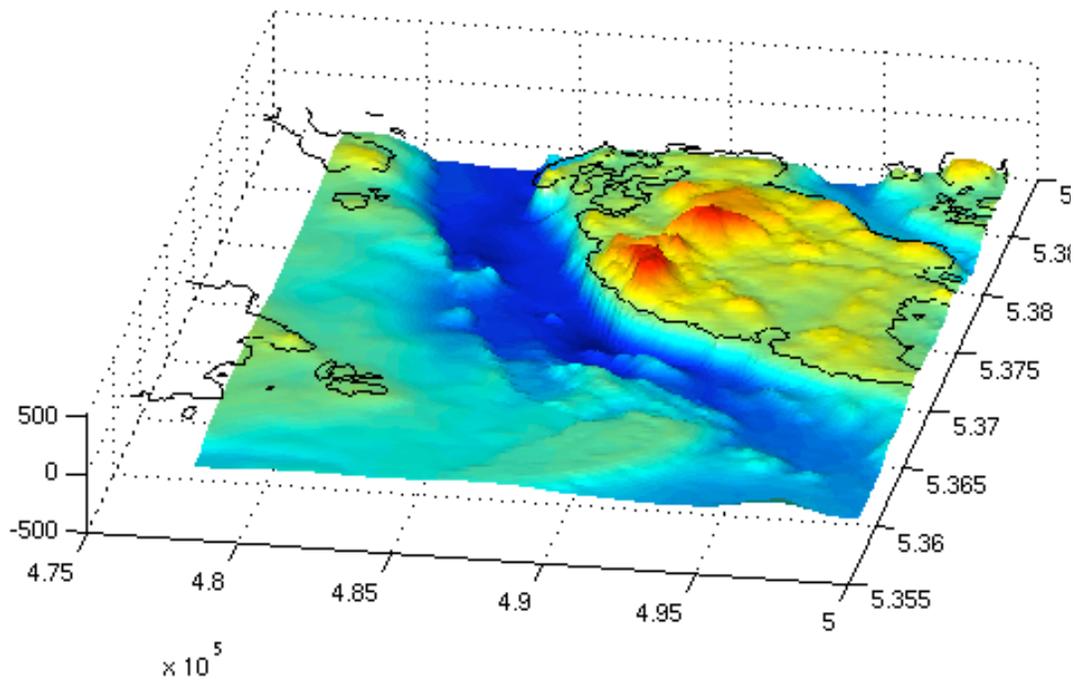

Figure 2.1 Perspective view of Haro Strait bathymetry

---

[7] www.ngdc.noaa.gov/mgg/bathymetry/relief.html and http://geopubs.wr.usgs.gov/open-file/of99-369/
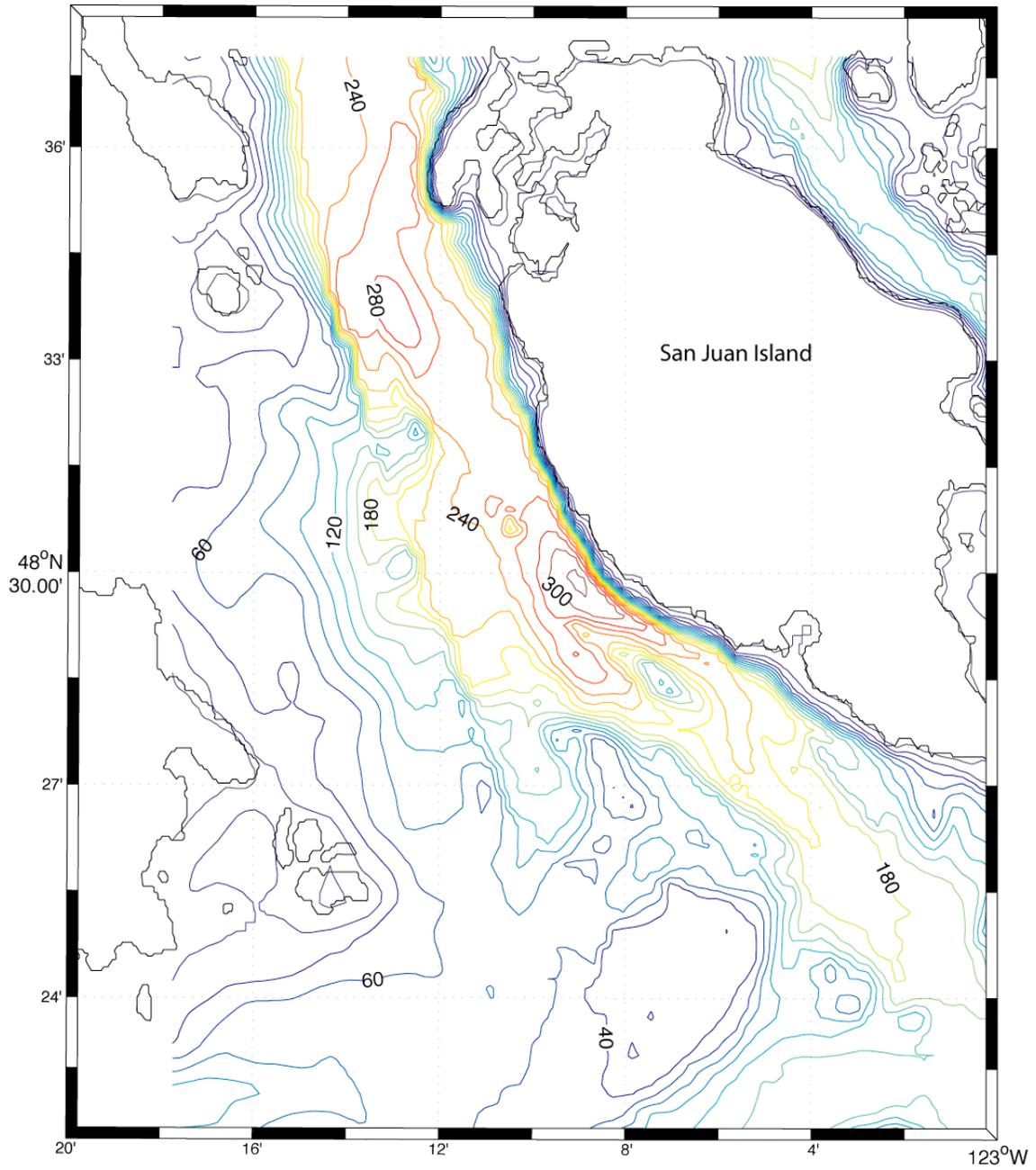
Figure 2.2 Bathymetry of Haro Strait, 20-m contours

2.2.   Geo-acoustic parameters

Haro Strait was formed glacially. The steep walls about the west side of San Juan Island are exposed rock. Silt and sand material lie on the bottom of the channel, but because of the strong and variable currents, the thickness of this silty sediment layer varies temporally and spatially. More precise details of the bottom properties are known for very small sections of Haro Strait as a result of recent geo-acoustic inverse studies.[8] Here the bottom was surveyed using echo sounders, and sediment samples taken with grab samples and cores.

Because the bottom is likely variable and little data is available, we modeled the geo-acoustic environment with three different parameterizations, each within a bound we felt reasonable from the limited amount of geology known and measurements taken. Crudely speaking, the bottom acts as a sink of acoustic energy, with silt and sand absorbing much more sound energy than hard rock. The limiting cases are a thick layer of silt (thick compared to the wavelength of the sound waves) and exposed hard rock. In the case of hard exposed rock with large slopes, such as off the west coast of San Juan Island, backscattering and reverberation can be an important concern, but is beyond the scope of the present study. We also do not include erratic blocks in the geo-acoustic modeling as their population density is expected to be too low.

For the acoustic propagation model the relevant geo-acoustic parameters are 1) the sound speed profile, 2) the density profile of the bottom, and 3) bottom attenuation profile. Because we are mainly concerned with the deep channel of Haro Strait, we assumed a nominal sediment thickness of twenty-five meters and used a critical slope of fourteen degrees to set the bottom type to either a sand-mud-gravel composition or exposed rock. If the slope of the bottom (determined from the bathymetric data described in Section 2.1) is greater than this critical slope, we assumed the bottom would be scoured by the strong tidal currents so that it would remain as exposed rock. Otherwise the material is assumed to be a layer of sand, gravel, and mud. (Tables in Section 5.2 summarize the geo-acoustic parameterization used for the modeling.)

2.3.   Sound speed profiles

Conductivity, temperature, and depth (CTD) data were collected over many years in the Haro Strait region. We obtained this data for the last twenty years from DFO-Canada (J. Linguati, Ocean Science and Productivity Division, Fisheries and Oceans Canada, personal communication, 2004). There were seventy CTD locations for the months of

---

[8] Chapman, N.R., L. Jaschke, M. McDonald, H. Schmidt, and M. Johnson, 1997. "Matched field geoacoustic tomography using light bulb sound sources," *Proceedings Oceans '97*, MTS/IEEE, pp 763–768.

May and June, the period during which the acoustic data were collected (Figure 2.3). Of these CTD locations, only locations that were within 15 km of the receiver location were used to produce sound speed profiles according to the equation of state given by Del Grosso.[9] The resulting sound speed profiles from May and June data taken over a twelve-year span in Haro Strait show sound speed profiles nearly invariant in nature with both geographic location and depth (Figure 2.4). Seasonal variations exist (not shown), and may be of interest for future studies. Considering the short ranges of propagation (< 10 km) along with the very weak variation in the sound speed environment (< 0.5%), we feel justified in using a single sound speed profile of 1480 m/s for our propagation model (see Section 5).
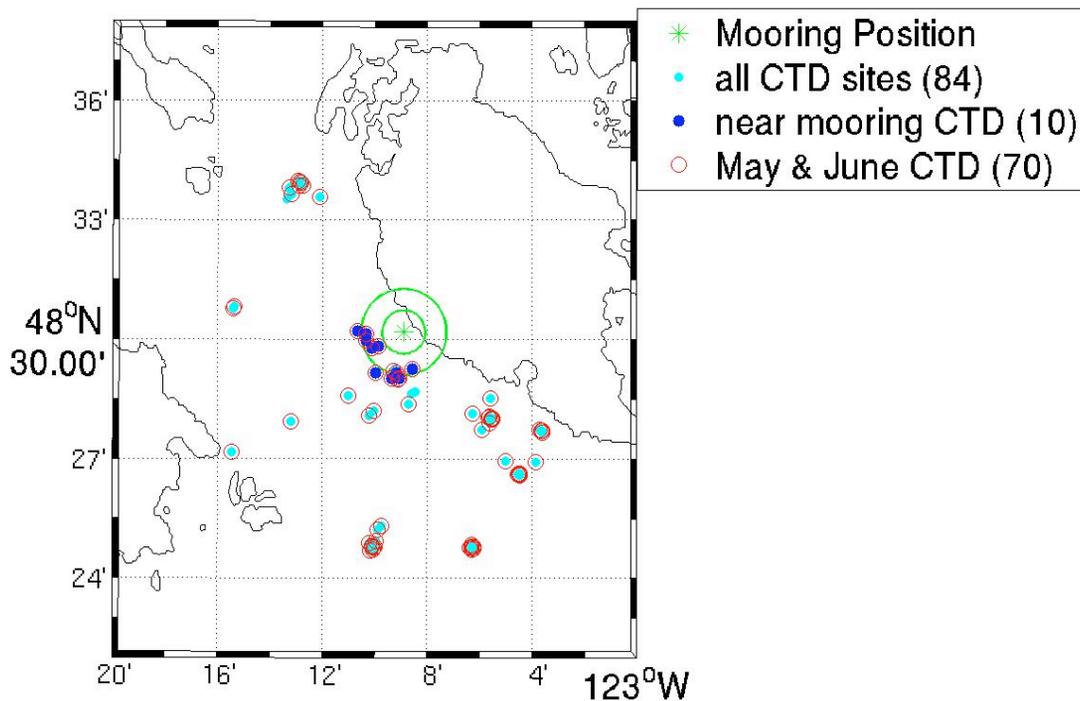
Figure 2.3 Map of Haro Strait showing positions where temperature and conductivity data (CTD) were collected

---

[9] Del Grosso, V.A., 1974. "A new equation for the speed of sound in natural waters (with comparisons to other equations)," *J. Acoust. Soc. Am.*, 56, 1084–1091.
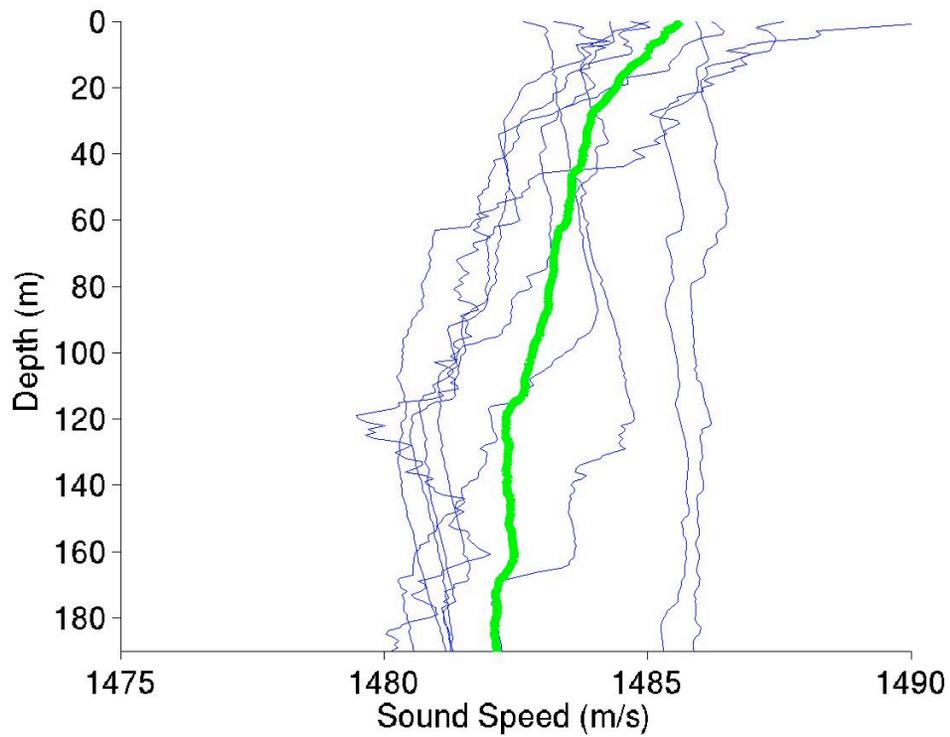
Figure 2.4 Sound speed profiles derived from CTD casts collected in May and June 1990–2002. Only profiles that spanned the full water column are show. The average of these profiles is shown in green.

3.   Ship Traffic

3.1.   Vessel Tracking System (VTOSS)

The Marine Communications and Traffic Services (MTS) of the Canadian Coast Guard operate the proprietary Vessel Traffic Operations Support System (VTOSS). VTOSS collects radar signatures of vessels greater than twenty meters long, providing position, course, and speed. The system also collects 'electronic handoff' data from vessels that are approaching within one hour of an exchange line or upon departure for vessels that are berthed one hour from an exchange line. The handoff data include the vessel name, call sign, type, number and type of barges (loaded or empty), port of origin and destination, speed, exchange line time of arrival estimate, and possibly additional information that might be useful to MCTS in regards to safe-guarding vessel traffic. Brian Bain, the Officer in Charge of MCTS Victoria, gave us permission to use data from radar signatures of ships that pass in the vicinity of Haro Strait.   Ian Wade (DFO, A/OIC Victoria MCTS Centre) provided an 'xbase database' file of vessel tracking data that we parsed for the data fields we desired. The database file contained a maximum of twenty-eight fields of data for ships operating in the Haro Strait region over the period of May 27 to June 30, 2004 (note May 26, June 9, 19, and 20 were not supplied due to software errors).

Typically, only 20 fields held data. Table 3.1 shows the field labels and two examples from two different ships. The first field signifies the date and time the radar signature was recorded; it is stored in the format 'yyyy mm dd hhmm' (year/month/hour/minute), and the signatures are recorded in six-minute intervals. Other fields we used were the ship name (field 3 in Table 3.1), the ship latitude and longitude (fields 17 and 18, respectively, in Table 3.1), and course and speed (fields 27 and 28, respectively, in Table 3.1).   The original data file was quite large of order 100 MB, so we separated it into smaller files according to the day. These were then filtered to obtain ship tracks, which were used for our data model comparisons (Section 5).

The VTOSS database comprises a relatively complete record of large ship traffic in the region. Figure 3.1 illustrates categorization of traffic by ship type during the period of interest (May 27 to June 30, 2004). Figure 3.2 illustrates the geographic sorting of vessel tracks by type during this same period. Figure 3.3 illustrates an estimate of the mean north and south shipping lanes for commercial cargo ships (not including tugs).

*Table 3.1 Examples from two lines of the VTOSS data file*

field #	Field label	example #1	example #2
1.	LAST_UDDTG	"200405170005",	"200405170005",
2.	VSL_ID	"CSTL19931231000495",	"CSTL19931231000494",
3.	NAME	"JACQUES CARTIER",	"CAPTAIN COOK",
4.	CALLSIGN	"CY6103",	"CY7903",
5.	LLOYDS_ID	"0314837",	"6613483",
6.	FLAG	"CA",	"CA",
7.	SATCOMNUM	"A",	"A",
8.	TYPE_ENC	,	,
9.	TYPE_DEC	"TUG",	"TUG",
10.	LOA	19.40,	22.90,
11.	GRT	72.00,	124.00
12.	TOW_ENC	"1HE",	"1 EMPTY BULK BARGE",
13.	TOW_DEC	,	,
14.	IS_DC	,	,
15.	IS_DD	,	,
16.	IS_SPI	,	,
17.	POS_LAT	49.42,	49.36,
18.	POS_LON	123.96,	123.90,
19.	POS_RDRDTG	"200405170005",	"200405170005",
20.	POS_CIP	,	,
21.	POS_CIPDTG	,	,
22.	POS_SRC	,	,
23.	CVTOSS_ZONE	"RDR",	"RDR",
24.	FROM_AT	"VIC",	"VIC",
25.	NEXT_TO	"LAF",	"LAF",
26.	SERVICE	"JER",	"MID",
27.	COURSE	251.00,	298.00,
28.	SPEED	15.6	8.3
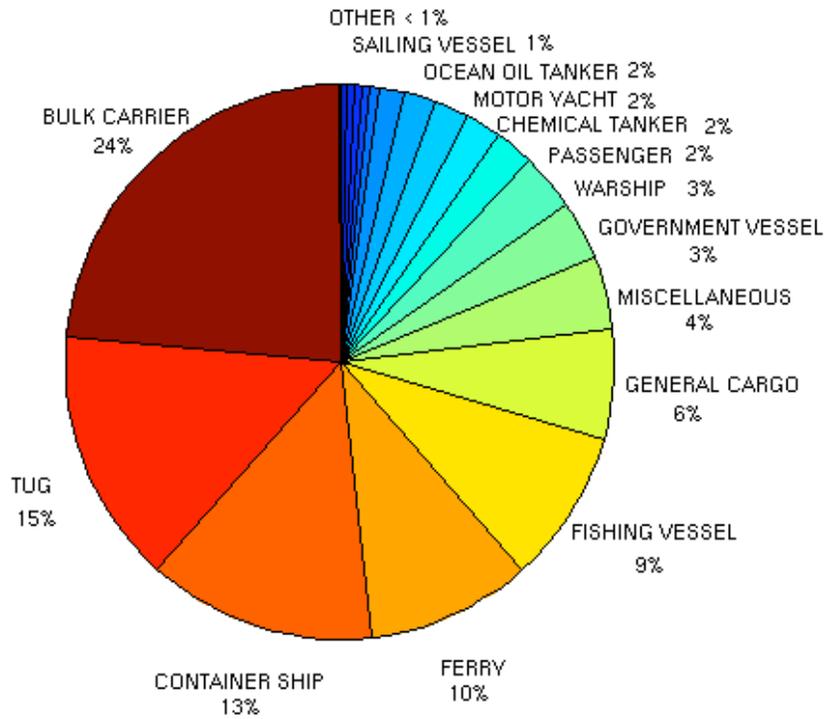
SHIP TYPE	COUNT	PERCENTAGE
BULK CARRIER	5090	23.6
TUG	3195	14.8
CONTAINER SHIP	2901	13.4
FERRY	2089	9.7
FISHING VESSEL	1920	8.9
GENERAL CARGO	1385	6.4
MISCELLANEOUS	929	4.3
GOVERNMENT VESSEL	730	3.4
WARSHIP	726	3.4
PASSENGER	494	2.3
CHEMICAL TANKER	465	2.2
MOTOR YACHT	433	2.0
SAILING VESSEL	410	1.9
OCEAN OIL TANKER	320	1.5
PLEASURE CRAFT	110	0.5
LOG SHIP	105	0.5
CHARTER VESSEL	98	0.5
COASTAL FREIGHTER	86	0.4
COMBINATION CARRIER (OBO)	64	0.3
FISH FACTORY	19	0.1
FISH PROCESSOR	5	0.0

Figure 3.1 Vessel types in Haro Strait derived from VTOSS for May 27 to June 30, 2004

Figure 3.2 (Following) Vessel tracks in Haro Strait derived from VTOSS for May 27 to June 30, 2004

VTS GENERAL CARGO Positions: days 148-182, 2004

VTS CONTAINER SHIP Positions: days 148-182, 2004

VTS FERRY Positions: days 148-182, 2004

VTS FISHING VESSEL Positions: days 148-182, 2004
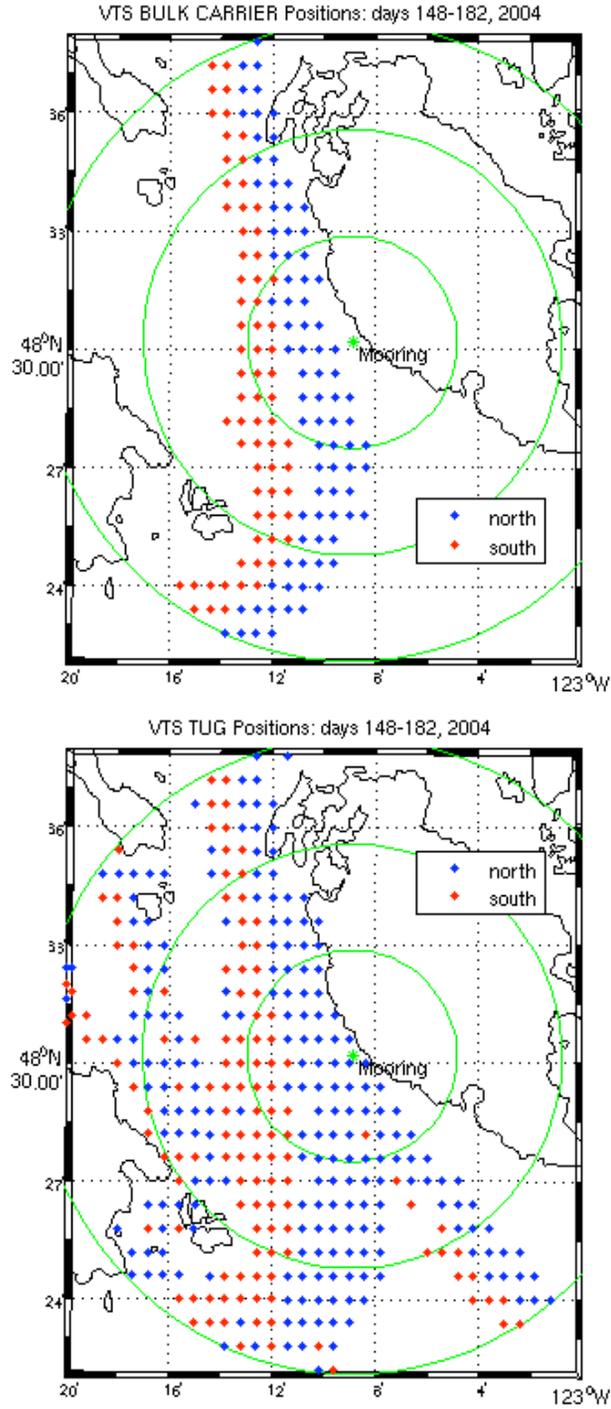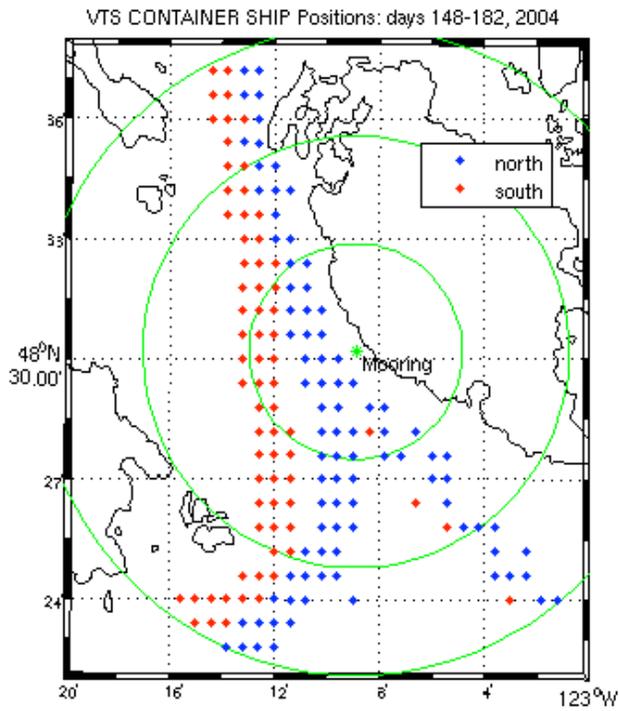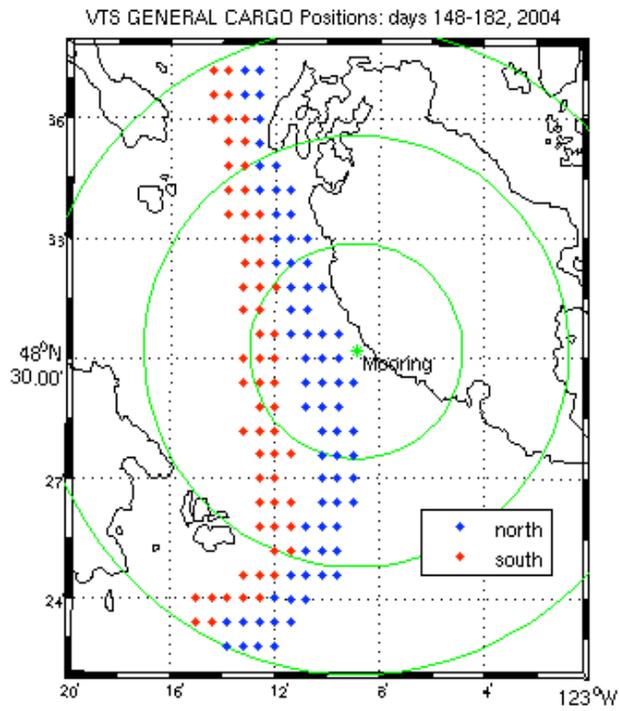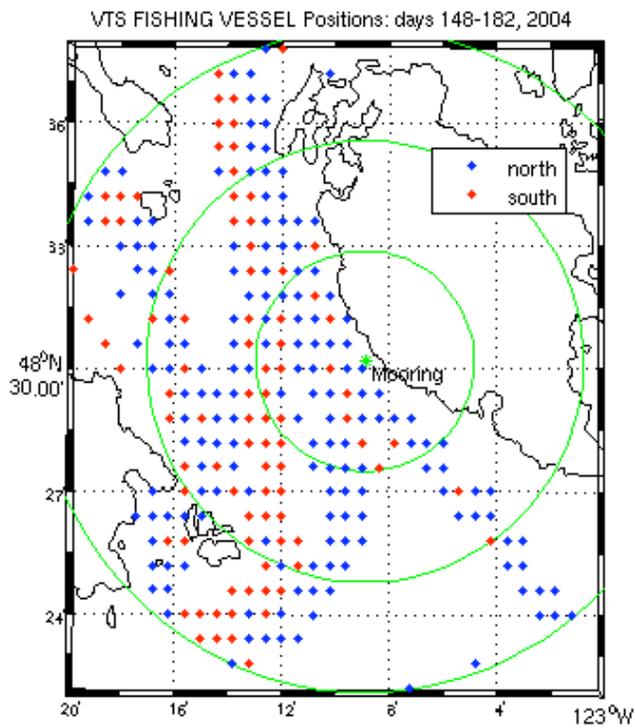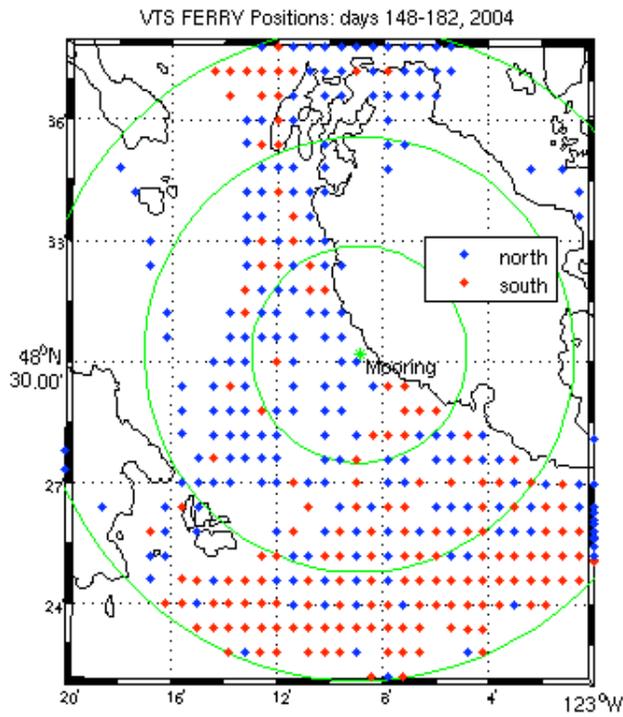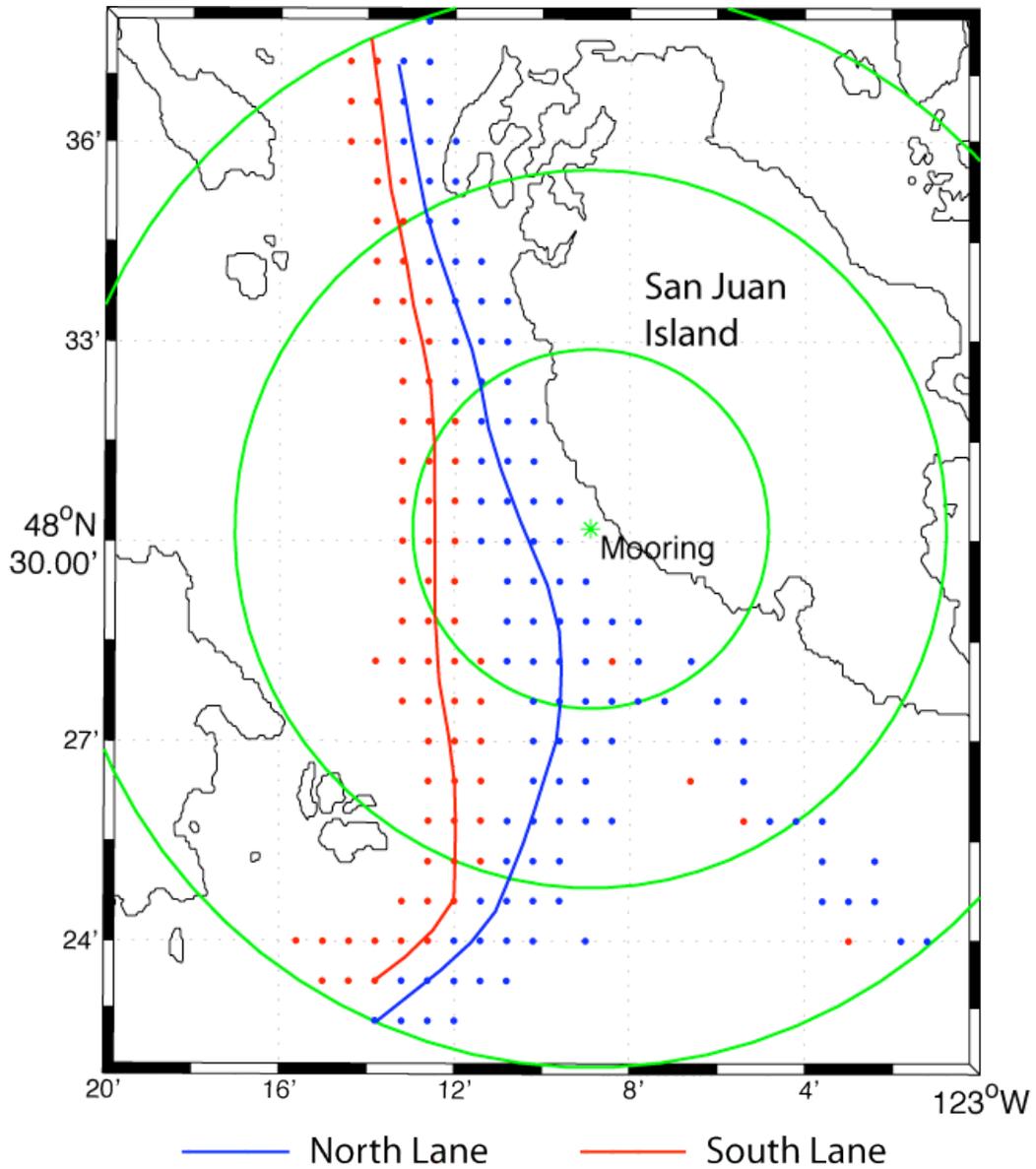
Figure 3.3 North and south commercial cargo shipping lanes in Haro Strait obtained from VTOSS data for May 27 to June 30, 2004

4. Measurements of Underwater Sound

4.1. Passive Aquatic Listerners (PAL)

Acoustic data used in this analysis were recorded with the Passive Aquatic Listeners (PALs). PALs are autonomous acoustic recorders designed to be attached to ocean moorings consisting of a broadband, low-noise hydrophone, a signal processing board, a low-power microprocessor with a 100-kHz A/D digitizer, a 2-GByte memory card and a 48-Amp-hour battery pack. A PAL is a cylindrical instrument 30 inches long by 6 inches in diameter. The hydrophone extends from one end. It is typically mounted in a cage to avoid damage by possible fishing lines. The weight in water is about 10 lbs, making it deployable on almost any type of mooring line. The new casings are more robust and will increase the weight to about 20 lbs in water.

A PAL is autonomous and depends on internal batteries for operation. The temporal sampling strategy is designed to allow the instrument to record data for up to one year.[10] To achieve this, the PAL enters a low-power ("sleep") mode between each data sample. The principal power usage is from the microprocessor when it is "awake," drawing 43 ma. The microprocessor needs to be in this mode for roughly 30 s for each sample. The microprocessor only draws 0.3 ma when "asleep." The hydrophone, pre-amp, and signal processing board draw 12 ma when "on" and 1 ma when "off." These only need to be "on" for about 2 s per sample, and so the power cost of each sample is 3.8 x 10^{-4} Amp-hours. The total power cost of the expected 100,000 samples during a one-year deployment is roughly 42 Amp-hours. This power demand is met by using three stacks of 10 alkaline D-cell batteries, each with 1.6 Amp-hours of energy, a total of 48 Amp-hours. Data storage capacity is met using 2-GB flash memory cards.

Figure 4.1 PAL in deployment cage

PAL electronics consist of a low-noise wideband hydrophone (either an ITC-8263 or a Hi-Tech-92WB), signal pre-amplifiers, and a recording computer (Tattletale-8). The nominal sensitivity of these instruments is –160 dB relative to 1 V/μPa and the equivalent oceanic background noise level of the pre-amplifier system is about 28 dB relative to 1

---

[10] Ma, B., and J.A. Nystuen, 2005. "Passive acoustic detection and measurement of rainfall at sea," *J. Atmos. Ocean. Technol.*, 22, 1225–1248.

$\mu Pa^2 Hz^{-1}$. Band-pass filters are present to reduce saturation from low-frequency sound (high-pass at 300 Hz) and aliasing from above 50 kHz (low-pass at 40 kHz). The hydrophone sensitivity also rolls off above its resonance frequency, about 40 kHz. A data collection sequence consists of a four-second time series collected at 100 kHz. This time series is then sub-sampled at four times, generating four 1024-point or 10.24-ms short time series. Each of these sub-samples is fast Fourier transformed (FFT) to obtain a 512-point (0–50-kHz) power spectrum. These four spectra are averaged together and spectrally compressed to 64 frequency bins, with frequency resolution of 200 Hz from 100–3000 Hz and 1 kHz from 3–50 kHz. These spectra are evaluated individually to determine the acoustic source and then are recorded internally. The time interval between data collection sequences is variable depending on the acoustic source detected and the mission requirements.

The PAL is not a continuous acoustic sampler. The basic PAL data are a time series of spectral levels between 200 Hz and 50 kHz. The interval between samples is chosen by the user depending on the intent of the deployment. Typically this interval is several minutes, but is variable depending on the sound source detected. Between data samples, the PAL processor enters a deep sleep mode to conserve batteries.

4.2.   PAL deployment in Haro Strait

A PAL was deployed in Haro Strait for a 6-week period in early summer of 2004 (May 27 to July 2004). The mooring was located along the western coast of San Juan Island in approximately 300 m of water [48°30.186'N, 123°08.896'W], as shown in Figure 4.2. The PAL was attached to a bottom mooring with the recording hydrophone at an approximate depth of 100 m below the surface. The mooring configuration is illustrated in Figure 4.3.
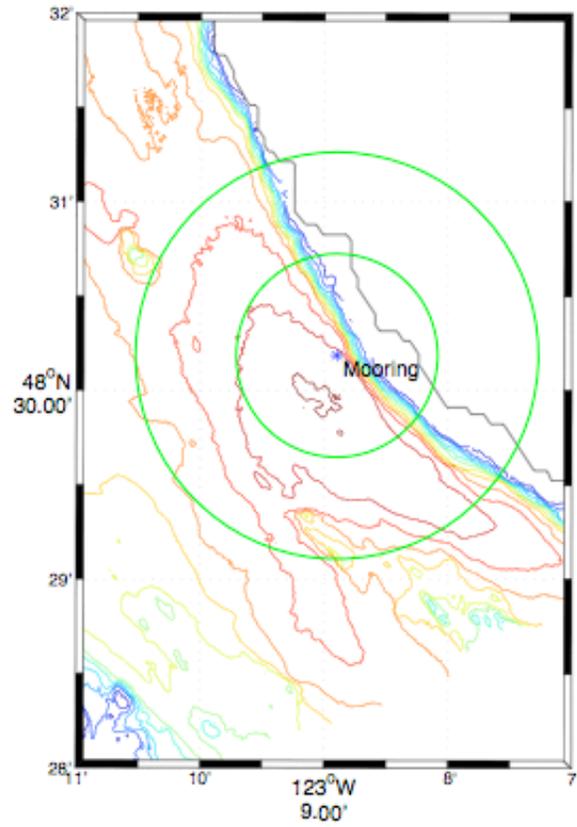
Figure 4.2 Position of PAL deployment in Haro Strait, 50-m depth contours shown

Haro Strait PAL Mooring
as Deployed, May 27, 2004

48° 30.186' N, 123° 08.896' W, 167 fathoms (Chart)
Not to Scale – June 24, 2004 KH

95 m — ⌀ 12" Sphere

⌀ 12" Sphere

109 m — PAL (Nystuen, APL-UW)

168 m (550 ft) 3/8"
polypropylene line

278 m — 31" Syntactic sphere

31" Syntactic sphere

294 m — HARP

Dual EG&G
Acoustic Releases

305 m — Anchor
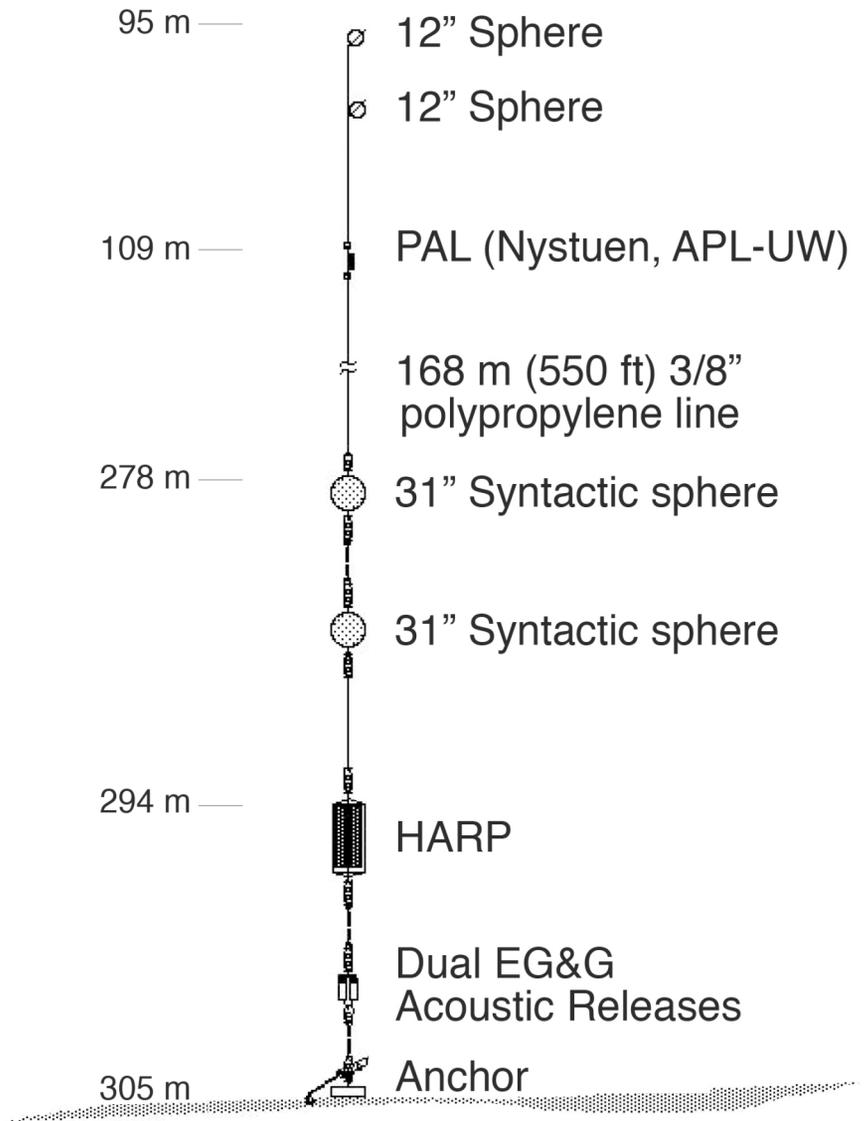
Figure 4.3 Haro Strait mooring configuration

4.3. Ship signatures

The time-frequency data provided by the PAL recordings reveal a variety of acoustic signatures that are likely representative of the underwater acoustic environment of Haro Strait. Because the data available for this study were recorded in the form of time averaged spectra, the data do not typically show transient acoustic signals of duration on the order of ~5 s or less, such as individual whale vocalizations. However, the data do show (as designed) longer time scale features such as the acoustic signatures of passing ships and natural sound sources such as wind and rail. In this sense, the PAL data is representative of persistent background sound levels that an animal would experience in a particular area and at a particular depth.

Consider the spectrogram recorded by the PAL instrument for a single day (day 151) (Figure 4.4) that represents a typical day during the deployment period. During the daylight hours increased acoustic activity is observed as the density of spectral lines increases relative to the density during nighttime. Ships and boats are likely the primary source of background sound levels. Ship traffic also continues during nighttime hours. Larger ship signatures are characteristically louder at lower frequencies with broad spectral bandwidths. The higher frequency content of the ship signatures is typically lower for ships at longer ranges from the receiver, as higher frequencies will attenuate more with range. In general, however, the acoustic signatures of ships are complex and can vary greatly with ship type, speed, and orientation.[11] Other sound sources, for example, a signature of rain noise at 10–40 kHz at around 5:00 am (circled), are also observed in the spectrograms (Jeff Nystuen, APL-UW, personal communication, 2005).
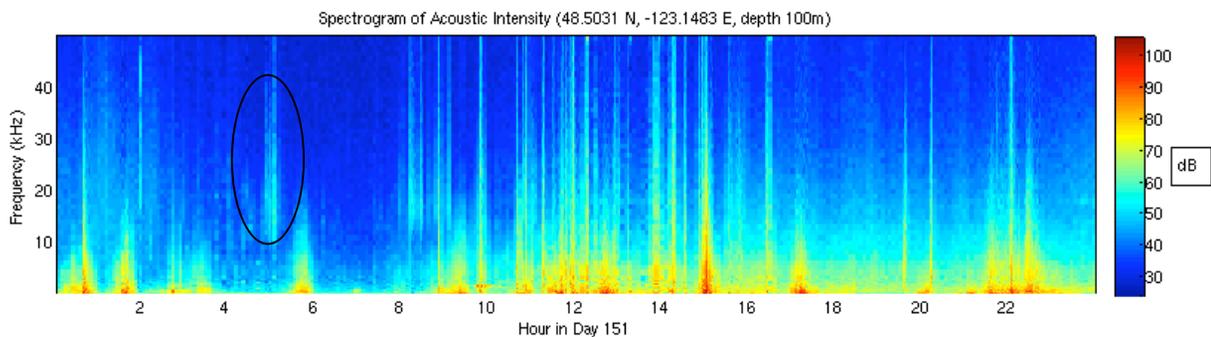

Figure 4.4 PAL data for a single day

---

[11] Urick, R.J., 1983. *Principles of Underwater Sound,* McGraw-Hill, 1983.

Of particular interest in the PAL data is the correlation of specific acoustic signatures with ship tracks provides by the VTOSS database. This allows the correlation of specific acoustic recording with the ship type, location, speed, and orientation. The recorded signatures of identified ships can then be used (in combination with propagation modeling) to infer absolute ship source levels and their contribution to background sound levels in particular areas (analysis discussed in the following sections). Several examples are discussed here to illustrate the methodology of ship source analysis.

Example 1: Cargo ship passing within 1 km of mooring

The signature of a ship passing close to the mooring is characterized by higher received levels with an increase in the higher frequency content of the signal. It should be noted that the characteristics of a specific signature (spectral level and content) include both propagation effects and the unique spectral signature of the source. Different ships have different spectral signatures that are a function of speed and orientation. However, in general higher frequencies tend to attenuate more with range.

In this example a single ship track and acoustic signature is isolated. The spectral signature is shown (circled) in the PAL spectrogram (Figure 4.5). The associated VTOSS ship track (Figure 4.6) shows that the ship passed within 1 km of the mooring at approximately 15:00 on day 151, 2004. The spectral signature as a function of time (as the ship passes) for two frequencies of interest (3.6 kHz and 10.4 kHz) are also shown.
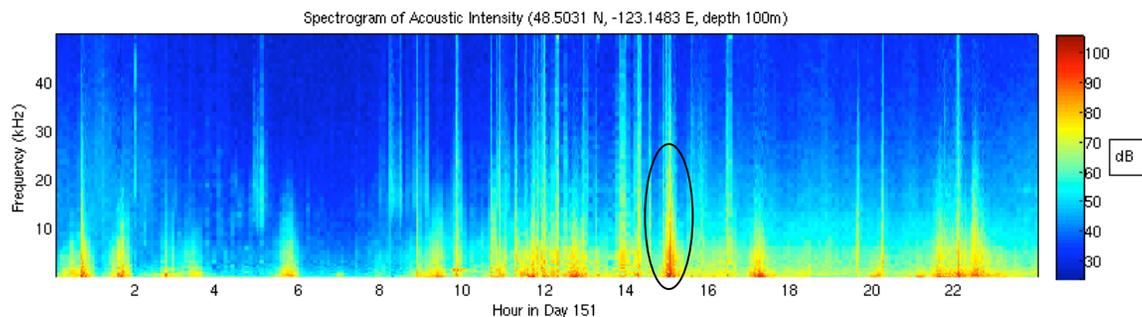

Figure 4.5 PAL data for a single day, with cargo ship identified (ellipse) from VTOSS data at hour 15 (3:00 pm)
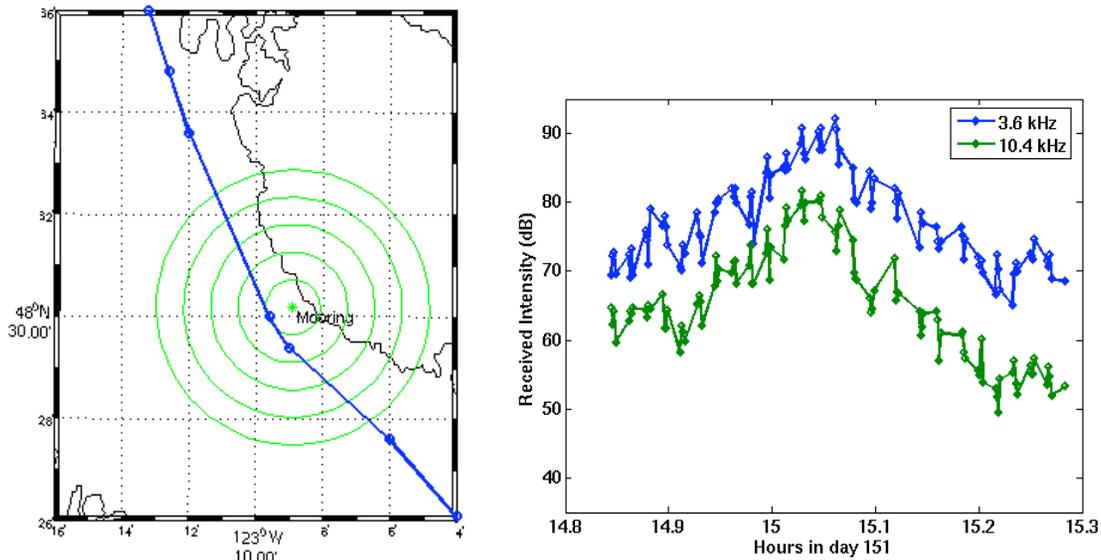
Figure 4.6 (left) Track of a cargo ship (blue) derived from VTOSS data in the vicinity of the PAL mooring (green star). Concentric circles about the mooring of radii 1, 2, 3, 4, and 5 km are shown in green. (right) PAL intensity data for two particular frequencies over the time interval when the cargo ship was in the vicinity of the mooring.

Example 2: Cargo ship passing at a range of ~5 km from mooring

The signature of a ship passing at a larger distance from the mooring is characterized by lower received levels with less higher frequencies in the signal. In this example the ship track and acoustic signature are also isolated, and the spectral signature is delineated (Figure 4.7).
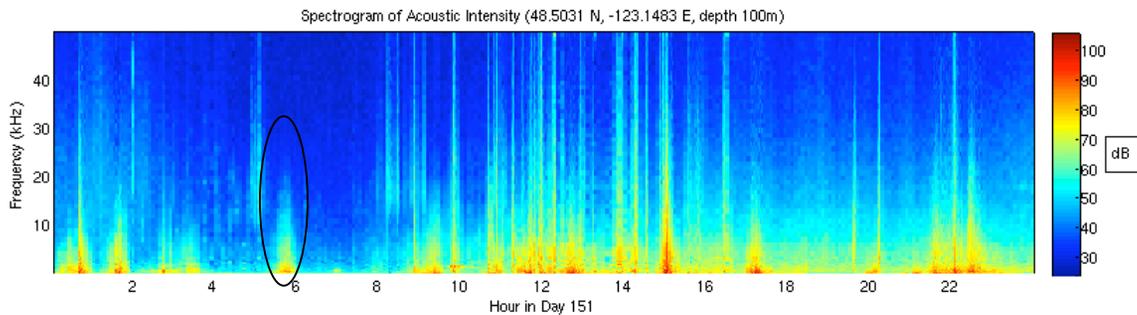

Figure 4.7 PAL data for a single day, with cargo ship identified (ellipse) from VTOSS data near hour 6 (6:00 am)

The associated VTOSS track of this ship is shown in Figure 4.8 where the ship passed within minimum range of 4–5 km of the mooring at approximately 05:45 on day 151, 2004. The spectral signatures as a function of time for two frequencies of interest (3.6 kHz and 10.4 kHz) are also shown. Note that the spectral levels at the same frequencies are approximately 20 dB/Hz lower compared with a ship passing at a distance of 1 km. Note also that the spectral signal shows much less variability.
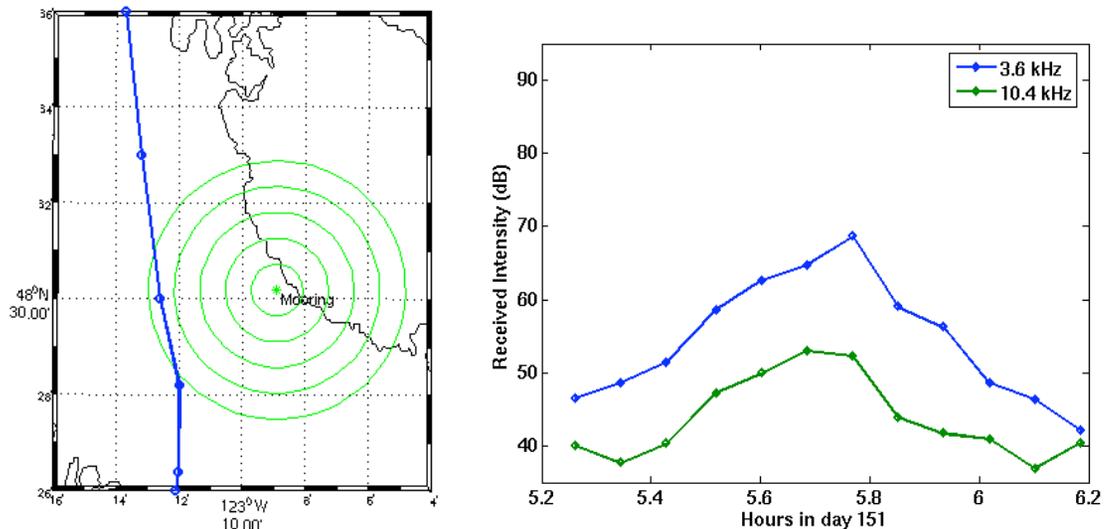

Figure 4.8 (left) Track of a cargo ship (blue) derived from VTOSS data in the vicinity of the PAL mooring (green star). Concentric circles about the mooring of radii 1, 2, 3, 4, and 5 km are shown in green. (right) PAL intensity data for two particular frequencies over the time interval when the cargo ship was in the vicinity of the mooring.

5. Acoustic Propagation Modeling

Simulations of acoustic propagation can be used to estimate acoustic transmission loss and variability associated with a particular source and receiver location. PAL recordings provide the underwater sounds levels received at a specific location and time due to unknown sound sources. The VTOSS database provides a record of locations and times of the sound sources (the larger ship traffic, at least) but no direct information about their acoustic signatures and source levels. Simulations provide a mechanism to combine these data (recordings and ship tracks) to estimate the source levels of the individual ship tracks.

5.1. Model description

The acoustic propagation model used here is a slightly modified version of the parabolic equation (PE) model that is part of the Navy's Oceanographic and Atmospheric Master Library (OAML). The modified version we use allows for a rough surface, which can be important for higher acoustic frequency (> 1 kHz) signals. This model assumes an isotropic spreading of acoustic energy in azimuth about a locally cylindrical coordinate system with axis of symmetry running vertically through the horizontal position of the acoustic source (a ship). The model also assumes acoustic energy only propagates away from the source, and backscattering is neglected. These two approximations are reasonable for most situations and for this study.

There are expected to be regions near the west coast of San Juan Island with significant backscatter from the sloping walls. These regions are very difficult to model because: 1) efficient full-wave numerical models that accurately describe the backscattering are not readily available for the range scales of interest, and 2) the bottom properties are extremely difficult to obtain at the necessary resolution to perform accurate model predictions. There are methods to resolve these, but they lie outside the scope of this report. (A methodology to address this issue in a future study is proposed in Section 6). We feel that the PE model is appropriate here because most of the propagation modeling is constrained to the channel, and the sound that has interacted with the steep canyon walls will be significantly lower in intensity compared with what has propagated from a ship source in the channel.

Like all PE models, the basic equation solves an approximation to the Helmholtz wave equation, whereby one assumes that the envelope of the evolving acoustic pressure field varies slowly on the order of the acoustic wavelength. This allows a one-way wave equation for the envelope of the acoustic pressure field, which can be solved numerically as an initial value problem. The standard boundary conditions are pressure equal to zero

at the surface and the normal derivative of the pressure equal to zero at the computational bottom. Note the computational bottom is often hundreds of meters greater than the ocean bottom to allow for sediment and basement interactions, and the bottom is treated as a fluid. A profile of sound speed is required in the ocean volume domain, and a profile for sound speed, density, and attenuation is required at and below the ocean–sediment interface. The frequency dependent attenuation due to boric acid and magnesium sulfate ionic relaxation processes, which are significant at acoustic frequencies at and above one kilohertz, are automatically handled within the model.

Particular features addressed by the model are rough surface and rough bottom scattering. Rough bottom scattering is handled by modifying the bathymetric database (Section 2.1) to include random displacements at horizontal scales of the order of 1 m. The rough surface is addressed similarly, but the random surface displacements are treated more physically, by creating realizations based on their spectral characterization from wind forcing. The surface is considered frozen in the model, which is a valid approximation because the phase speed of the acoustic waves is much greater than that of the surface waves. Also, because the model treats the bottom and surface as deterministic, one cannot expect point-wise convergence between the model and data; i.e., we can only obtain realizations of the bottom and surface that are statistically similar to what actually existed when the data were collected, so we can only expect statistical agreement between the model output and data. At lower frequencies of propagation, the effects of the rough surface and rough bottom become less important, and one might expect point-wise convergence to be obtained. However, at these lower frequencies (hundreds of Hz), the effects of the sub-bottom on the propagation become important, and little is known about the geo-acoustics of Haro Strait.

Finally, regarding the sub-bottom, the model allows for a jump in both density and sound speed at the water–sediment interface, and treats the sub-bottom as a fluid (shear waves are ignored). The sound speed in the sediment layer is allowed to increase linearly with depth, and a frequency dependent bottom loss is included. The thickness of the sediment layer is allowed to vary with range, independent of the bathymetry, and a highly absorbing basement layer is modeled below the sediment. Collins[12] and Rosenberg[13] both give a thorough explanation of the PE model used in this study.

---

[12] Collins, M.D., 1995. *User's Guide for RAM Versions 1.0 and 1.0p*, Naval Research Laboratory, Washington, D.C.
[13] Rosenberg, A.P., 1999. "A new rough surface parabolic equation program for computing low-frequency acoustic forward scattering from the ocean surface," *J. Acoust. Soc. Am*. 105, 144–153.

5.2. Model inputs

Because the environment is not well characterized in the Haro Strait region, simulations are performed for a realistic range of input values. In effect this provides bounds on the model outputs, given the uncertainty of the inputs. Model inputs consist of
1) Geo-acoustic parameters of the seafloor
2) Sound speed profiles of the water column
3) Bathymetry and bottom roughness
4) Sea surface roughness (due to wind)

5.2.1. Geo-acoustic parameters of the seafloor

For the region of interest, the geo-acoustic parameters of the seafloor are the least well characterized of the model inputs. Two bottom types are assumed: 1) mixed sand/mud sediment, and 2) mixed rock/sand sediment.

Table 5.1 Geo-acoustic parameters used for PE modeling in Haro Strait

Geo-acoustic Parameter	Sand/Mud	Rock/Sand
Sound speed (m/s)	1550	1800
Sound speed gradient	2	0
Density (g/cc)	1.7	2.0
Attenuation (dB/lambda)	0.129	0.7

5.2.2. Sound speed profile

The sound speed profile for the region is assumed to be linear with sound speed of 1483 m/s at the surface and 1480 m/s at the bottom. These values are taken from the mean sound speed profile (Section 2.2).

5.2.3. Rough sea surface and sea bottom

Randomness in the medium is modeled as surface roughness at both the sea surface and the sea bottom. Bottom roughness is generated using a power-law spectral model[14] with inputs defining the RMS height of the roughness and correlation length. Estimates of these parameters for Haro Strait are not available from measurements. Therefore, we estimated values based on similar types of bottoms. In all the cases shown we used a

---

[14] Jackson, D.R., K.B. Briggs, K.L. Williams, and M.D. Richardson, 1996. "Tests of models of high-frequency seafloor backscatter," *IEEE J. Ocean. Eng.*, 21, 458–470.

bottom RMS roughness height of 0.4 m and the bottom roughness correlation length of 10 m.

Sea surface roughness is generated using a Pierson–Moskowitz spectrum[15] spectral model for a one-dimensional surface with wind speed U (m/s) and parameters "alpha" and "beta." Three cases of sea surface conditions were considered: a flat surface (no wind); a typical sea surface with wind speed of 5 m/s; and a rough surface with winds of 10 m/s (Table 5.2).

Table 5.2. PE model parameters used to simulate realizations of a rough sea surface due to wind forcing in Haro Strait

Sea Surface Roughness Parameters	Flat	Typical	Rough
Wind speed (m/s)	0	5	10
Alpha	0	8.10e-3;	8.10e-3;
Beta	0.74	0.74	0.74

5.2.4. Monte-Carlo simulations

Inputs to the model that represent randomness in the environment require the generation of a statistical ensemble. The ensemble is used to describe the variability (e.g., mean and variance) in the model outputs due to the model inputs. For example, bottom roughness, when added to the propagation modeling, will create scattering at the sediment–water interface that will, in general, increase sound penetration into the seafloor, thus potentially increasing propagation loss between the source and the receiver. The addition of this type of randomness is an important aspect of the modeling effort. Statistical estimates are found using a Monte-Carlo method, in which multiple realizations of the surface roughness are generated for each source/receiver position and the model executed for each realization. Surface roughness realizations are generated by Fourier synthesis assuming Gaussian statistics for the roughness height.

Figure 5.1 illustrates the simulation output for one two-dimensional slice of the medium between the source (at a depth of 10 m in the upper left corner) and a grid of receiver positions along the propagation path. The upper surface in the plot is the sea surface (depth=0). The color scale represents acoustic intensity relative to the unit intensity source. The lower surface of the simulation illustrates the topography of the sea bottom, as the acoustic penetration into the bottom is highly attenuated, changing from higher

---

[15] Pierson, W.J. Jr., and L. Moskowitz, 1964. "A proposed spectral form for fully developed wind seas based on the similarity theory of S.A. Kitaigorodski," *J. Geophys. Res.*, 69, 5181–5190.

intensity (red) to lower intensity (blue). In this case the position of the source corresponds to the position of a ship, and the far right boundary of the grid corresponds to the position of the PAL mooring. The lower panel of Figure 5.1 illustrates the same simulation with bottom roughness added to the sediment–water interface, which increased randomness in the water and penetration into the sediment due to roughness at the sediment–water interface.

Monte-Carlo simulations provide an ensemble of transmission loss estimates for each source/receiver position and for a two-dimensional grid of values between the two positions. To compare model results with data (as discussed in the next section), descriptive statistics of the field at the receiver position must be evaluated. Here two measures are used: 1) the central tendency is defined in terms of the arithmetic *mean* and *median* of the field; and 2) dispersion of the model results is defined by the *interquartile range* (IQR). The IQR of the model is used to avoid imposing Gaussian assumptions on the model data variability. In general, one would expect to observe a Rayleigh (exponential) distribution for the values of the acoustic intensity due to randomness (surface roughness) in the propagation environment, at least in the limit of long range. However, for the limited number a realization used in the Monte-Carlo simulations (10 to 20), as well as the limited range, we found the IQR to be a more robust measure to highlight the variability of the acoustic intensity.

In addition to measuring dispersion of the model results over the Monte-Carlo realizations, the ensemble of output values is increased by considering a depth window for data analysis. In this case, all the grid values within a specified range of depths at the receiver location are added to the ensemble. There is considerable variability of the modeled intensity as a function of depth. Considering a window of depth (as opposed to a single depth value) also facilitates comparison of the model results with field data, as the precise depth of the PAL receiver is not known.
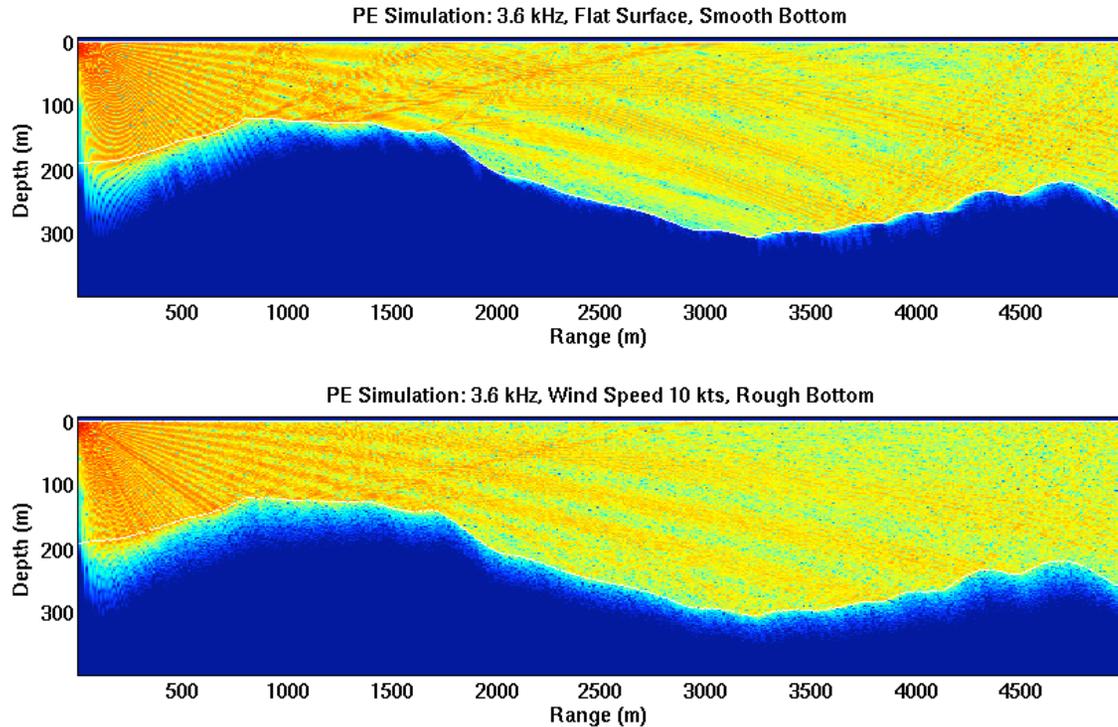
Figure 5.1 Comparison of transmission loss model results with and without sea surface roughness. Colors indicate intensity in dB, with red corresponding to high intensity and blue low. The dynamic range shown is 80 dB.

5.3. Model outputs

The propagation model provides an estimate of the propagation loss between a source and a receiver. The source is modeled as an omni-directional point source emitting a continuous (CW) signal at a single frequency. All the simulations in this analysis were performed at 3.6 kHz, chosen to match the frequency bin provide by the PAL data. The model output consists of a two-dimensional grid of sound pressure levels (relative to the unit source level) at discrete depths and ranges from the source position. The complex sound pressure level (p) output from the PE model is expressed as transmission loss using the sonar equation:

$$TL = 20\log(|p|) - 10\log(R),\qquad\qquad\qquad [5.1]$$

where R is the range from the source to the receiver. Given an estimate of TL, the actual sound level received at the receiver location is found by adding the source level (SL in dB) to the transmission loss.

5.4. Comparison of model results with field measurements

Simulations provide an estimate of the propagation loss between a source and a receiver (along with a measure of data dispersion). The measured field data provide absolute (calibrated) sound pressure levels received at a specific location in space and time. A comparison of model simulations and field data for known positions of acoustic sources (large ship tracks, in this case) can provide an estimate of the level of sound emitted at the source. Once confidence is gained in the modeling and measurement methodologies, the process of model/data comparison can be used to estimate the propagation of other sources of anthropogenic sound in the same area, to evaluate the potential variability of sound levels as a function of location and time (seasonal), and to eventually provide estimates of total shipping sound source levels in a limited region (such as in the main shipping channel).

This section provides a preliminary analysis of the model results compared with PAL data for the limited period of deployment of instruments in May–July 2004. The objective is to estimate the source levels of large ships in Haro Strait by comparing a variety of model results of propagation loss with recorded sound levels. The comparison is useful to evaluate applicability of model inputs and modeling strategies. Because the true ship source levels are not known, and in general are quite complicated, the estimates formed here are preliminary. Recommendations for further studies are given in Section 6.

5.4.1. Single ship comparisons

In cases where the acoustic signature of a single ship can be identified in the PAL data and the ship track identified by the VTOSS database, simulations of the propagation can be used to estimate the source level of the ship. (An example of this process is illustrated with a single ship in Section 4.3.)

Simulations are performed for 10 ship positions corresponding to 1-km range increments as the ship passed by the stationary mooring (Figure 5.2). Figure 5.3 illustrates the model results (intensity in dB) and the two-dimensional simulation geometry for each bathymetric slice between the source positions and the receiver. The source is located in the upper left corner of each slice, and the receiver is at the 100-m depth grid point at the right edge of the slice. The range between the source and receiver decreases and then increases as the ship passes the mooring.
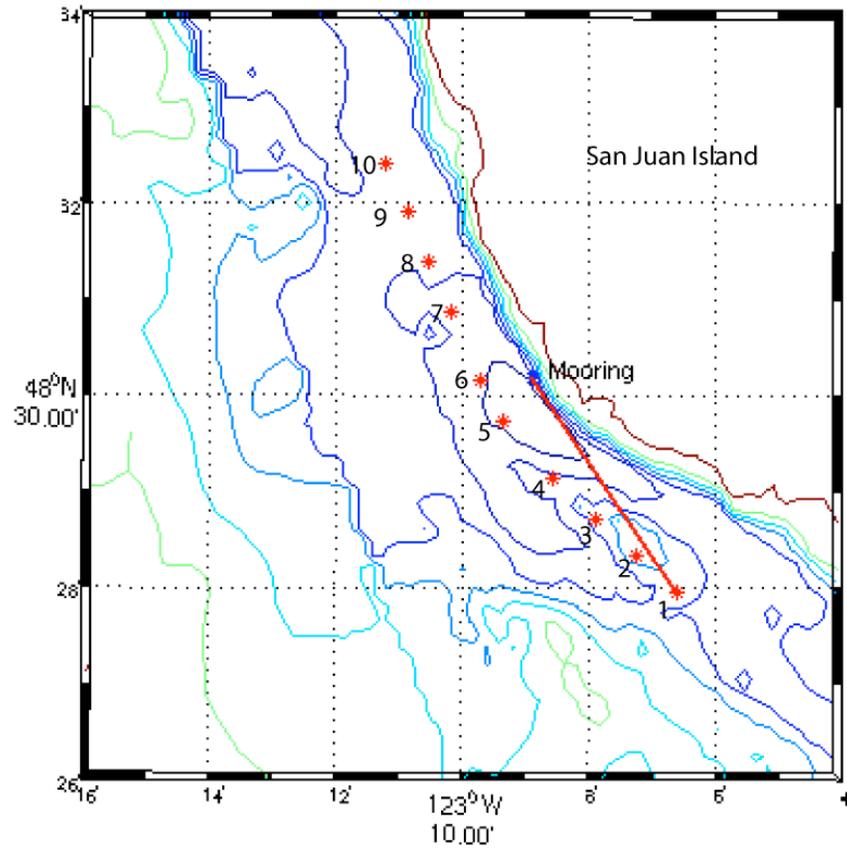
Figure 5.2 Source positions for VTOSS ship track named EverUnison corresponding to the source position in the TL plots show below. The red line shows the path associated with the first source position. Depth contours are at 50-m intervals.

Figure 5.3 (Following) Plots of transmission loss between the ship source positions (1–10) shown in Figure 5.2. Color scale represents the field in dB units with an 80-dB dynamic range.

Source Position 6: 3.6 kHz, Wind Speed 1 kts

Source Position 7: 3.6 kHz, Wind Speed 1 kts

Source Position 8: 3.6 kHz, Wind Speed 1 kts

Source Position 9: 3.6 kHz, Wind Speed 1 kts

Source Position 10: 3.6 kHz, Wind Speed 1 kts
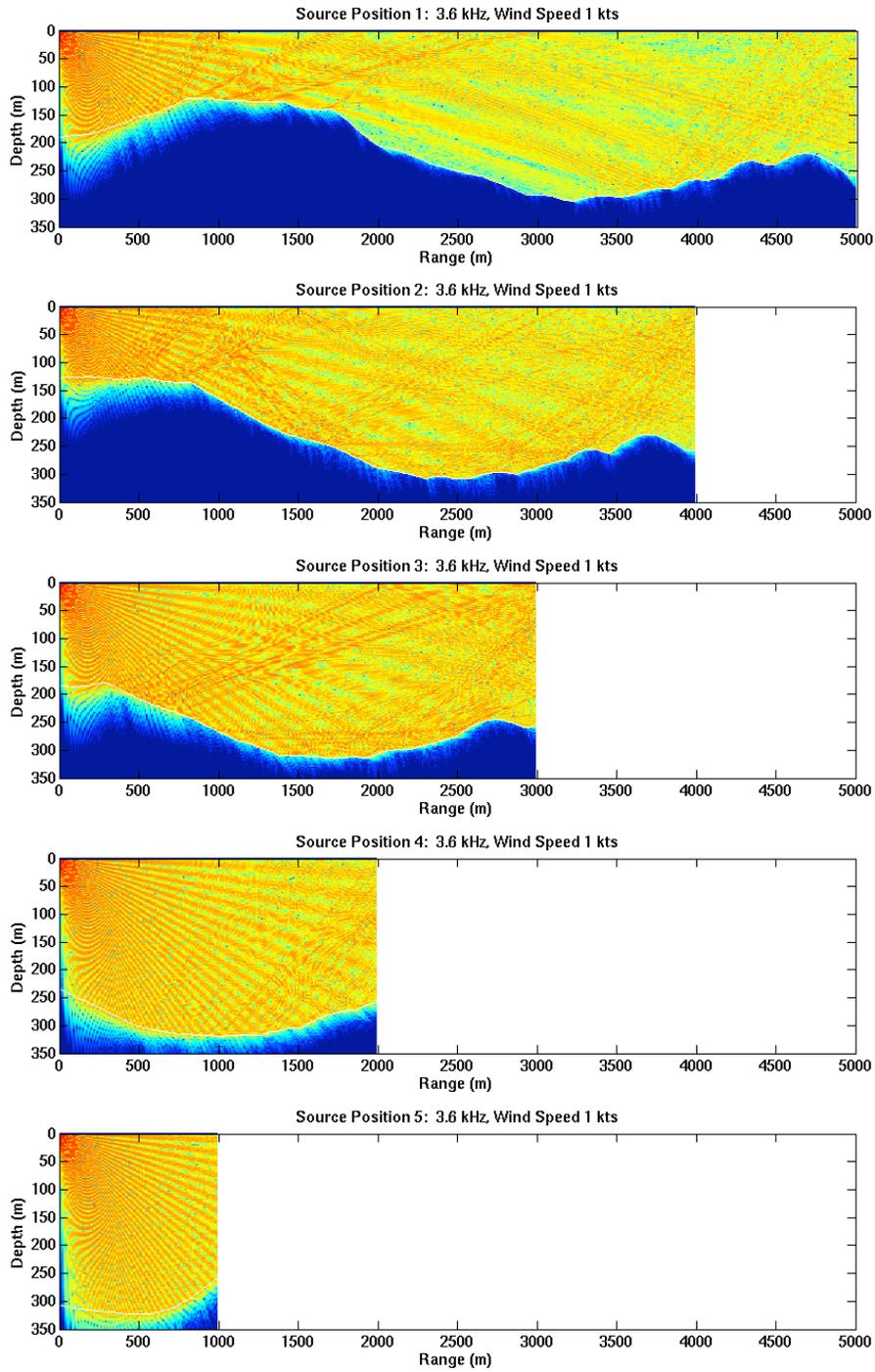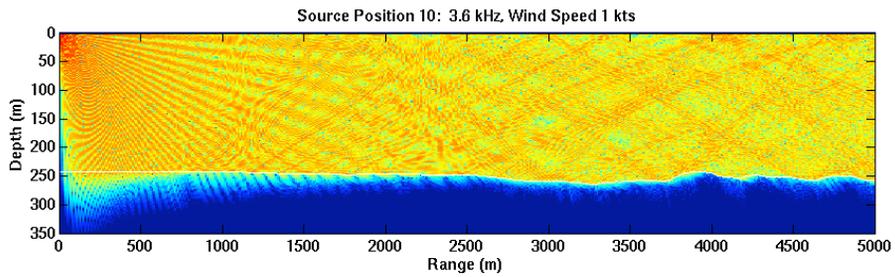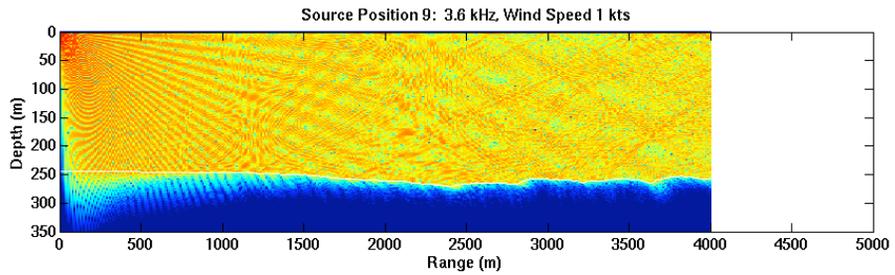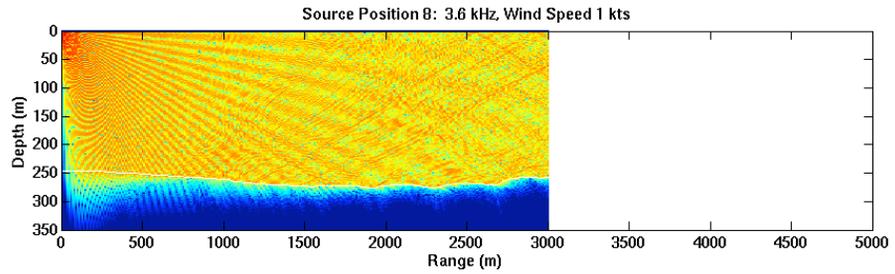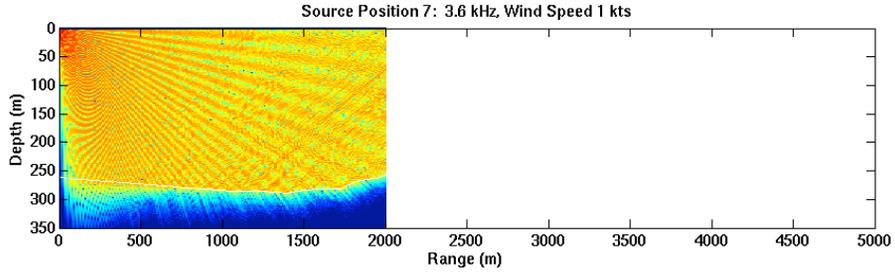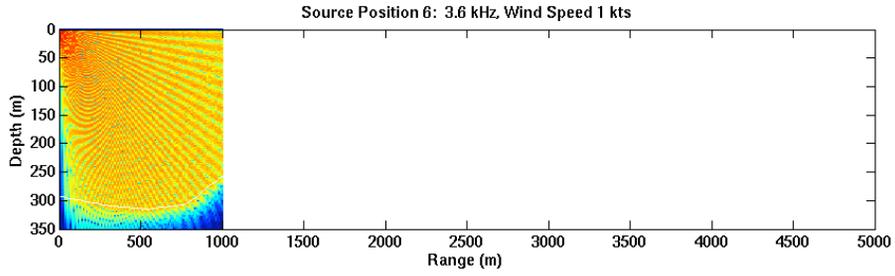
Propagation modeling is performed using Monte-Carlo simulations and bounds on the model inputs. To determine model sensitivity to different types of geo-acoustics parameters and wind speeds, multiple simulations are performed. The central tendency and dispersion of transmission loss are estimated for each case and results compared with measured data. For each case the transmission loss estimates are fit to the data to provide an estimate of the ship source level.

Figures 5.4, 5.5, and 5.6 illustrate the model/data fits and source level (SL) estimates for three cases: 1) smooth sand/mud sediment, 2) rough sand/mud sediment, and 3) rough rock/sand sediment. Each figure shows the model results for each source position as the ship passes by the mooring (10 positions total). At each source position three cases of wind speed (sea surface roughness) are simulated: 1) flat sea surface with wind speed 0 m/s, 2) rough sea surface with wind speed 5 m/s, and 3) rough sea surface with wind speed 10 m/s.

The model results are presented with the mean and median to express the central tendency of the simulated data and the IQR of the simulated data to express dispersion of the results. The IQR bounds represent the difference between the 75th and the 25th percentiles of the model data. Because of outliers in the data, the IQR was found to be more representative than the standard deviation as an estimate of the spread of the body of the data.

In all three cases of sediment type and wind speed the model results fit the measured results when an estimated ship source level of SL=175 dB was applied. In the last case (rough rock/sand sediment) the simulation results are high, implying that the transmission loss in this case is less than the other cases. This result is consistent with expectations as a rock/sand sediment type would be expected to attenuate sound propagation less than a sand/mud bottom type, in general. The results, however, are similar to within 3 dB for the various cases, implying that bottom type, sea surface roughness, and bottom roughness do not contribute greatly to the model results in this case. The propagation distances between the ship source and receiver may be so short that secondary effects of the bottom and surface conditions do not dominate the propagation loss estimates; bathymetry dominates.

The estimated ship source level of SL=175 dB @ 3.6 kHz is consistent with expected source levels for a large ship traveling at slow speed. These estimates cannot be verified because no independent measurements of source levels are available.

Variability in the model results is expressed in terms of the IRQ. In all three cases a range of values is on the order of 5 dB. Increased wind speed does not appear to increase variability. In the case of zero wind speed (flat sea surface), the observed variability is

due to windowing in depth (as opposed to multiple realizations), indicating significant fluctuation as a function of depth (relative to the variability caused by surface roughness).
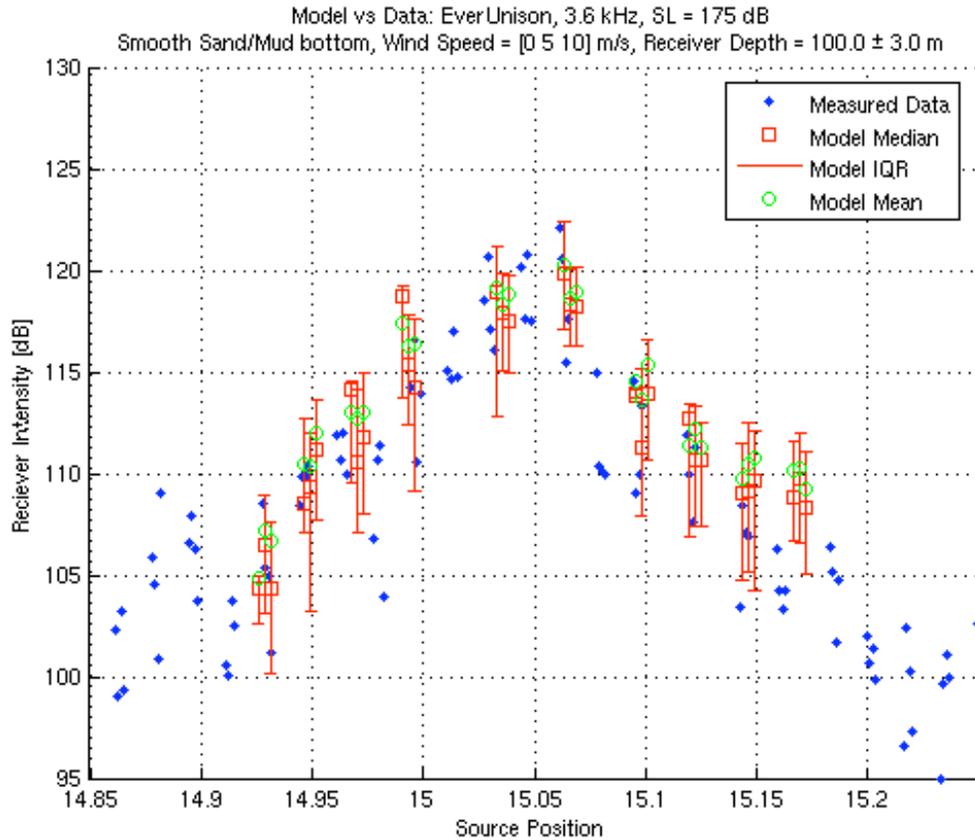

Figure 5.4 Comparison of model results and PAL data for a single ship track (EverUnison, day 151) with three wind speeds (0, 5, 10 m/s) and a smooth sand/mud bottom
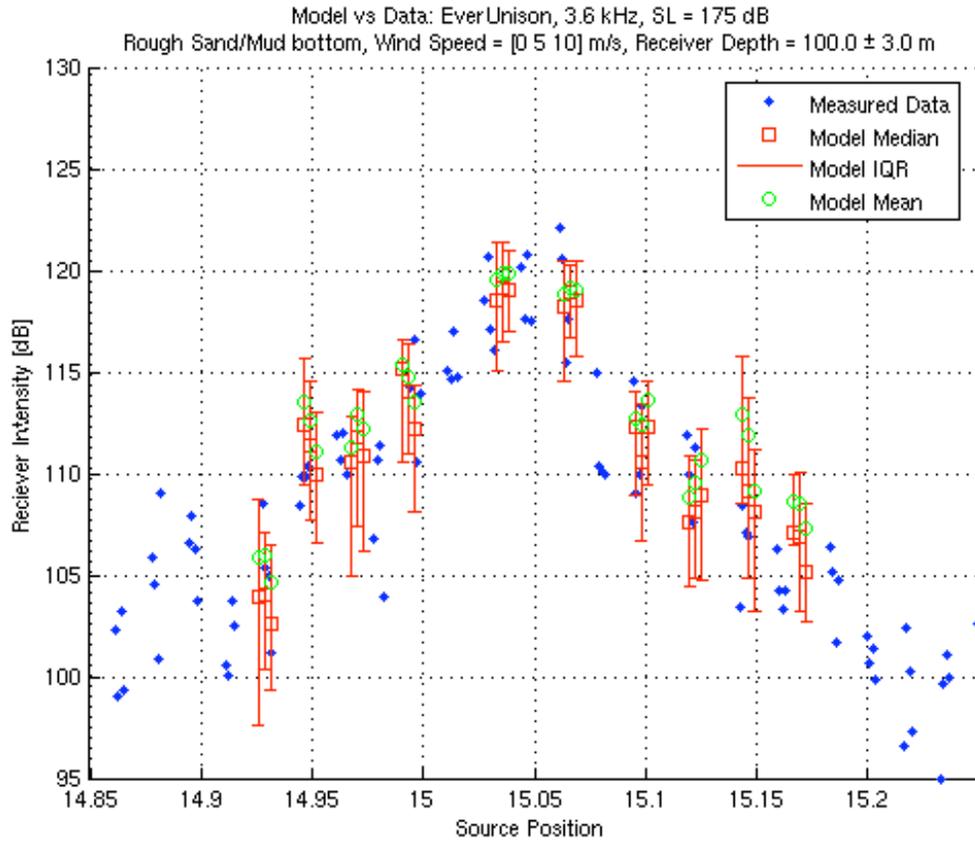
Figure 5.5 Comparison of model results and PAL data for a single ship track (EverUnison, day 151) with three wind speeds (0, 5, 10 m/s) and a rough sand/mud bottom
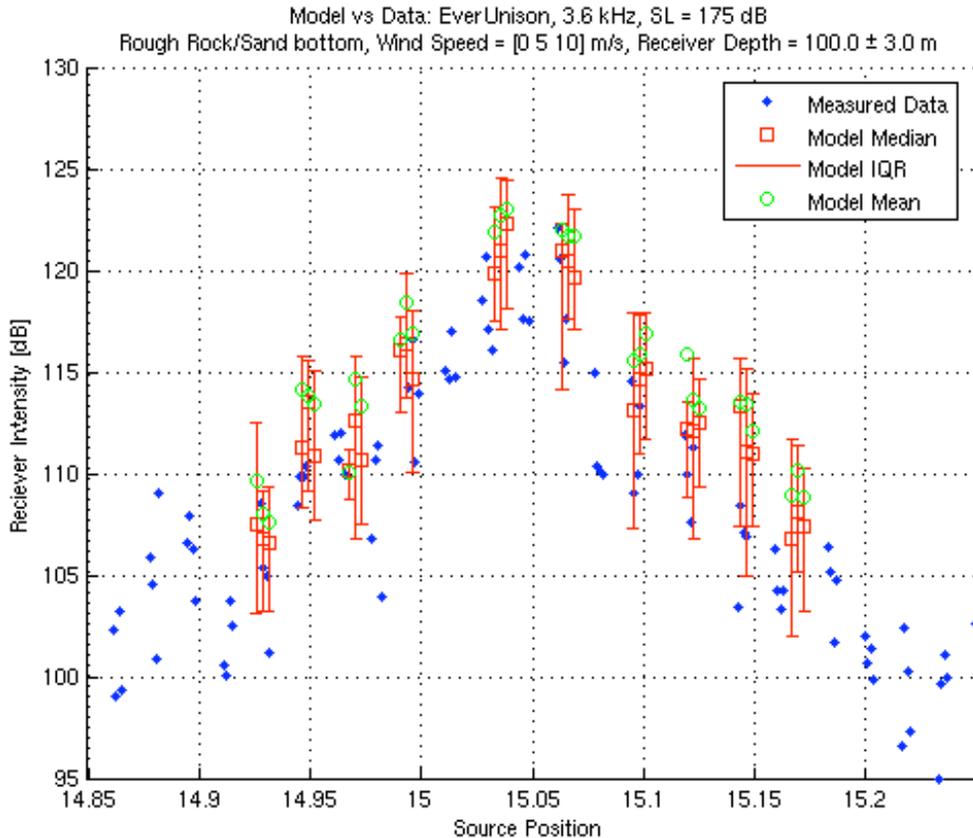
Figure 5.6 Comparison of model results and PAL data for a single ship track (EverUnison, day 151) with three wind speeds and a rough rock/sand bottom

5.4.2. Shipping lanes

The modeling strategy applied to an individual ship track can also be applied to the average positions of ships traveling in the major shipping lanes. Large commercial ships typically travel within a narrow lane north and south with a predictable track (Figure 3.3). The simulation of transmission loss for an average track along the shipping lane can be used to estimate ship source levels without performing a simulation of each individual ship.

In the case presented here, transmission loss estimates were formed for the northern ship lane derived from the VTOSS database for commercial cargo ships. Average ship positions along the center of the shipping lane are found at constant range increments of 1 km from the mooring location (Figure 5.7). At each position along the shipping lane Monte-Carlo simulations were performed for a 3.6-kHz source at 10 m depth. The geo-

acoustic parameters for these simulations were limited to rough sand/mud sediment type. As shown previously, the bottom type does not appear to be a major source of variability in the model results. Two wind speed values (5 and 10 m/s) were used to estimate a model central tendency and data dispersion.
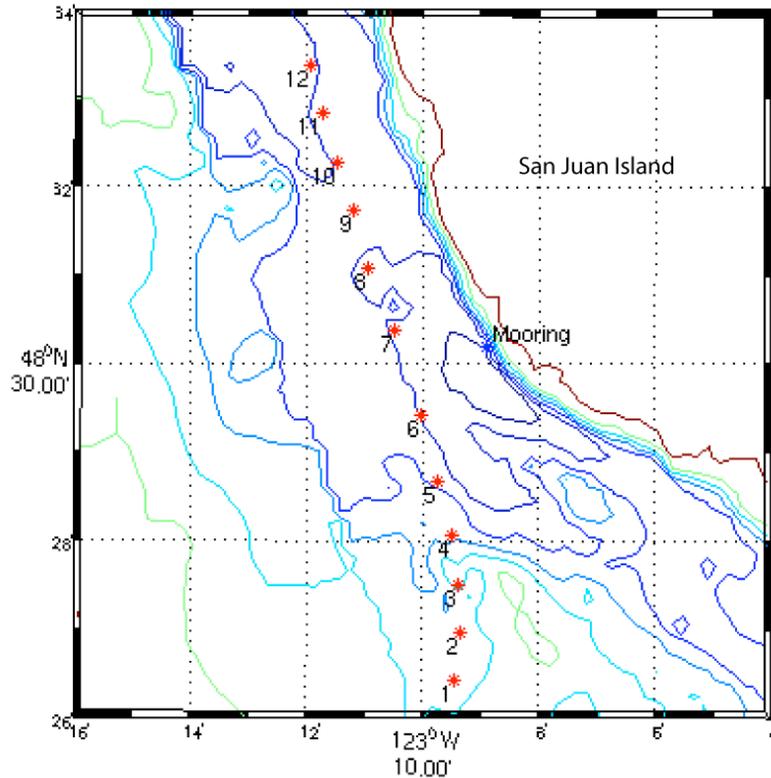

Figure 5.7 Source positions for the northern shipping lane derived from VTOSS ship tracks

Figure 5.8 illustrates the model results for transmission loss between ship positions in the shipping lane as the ship travels north past the mooring location. Source position numbers correspond to the position numbers in Figure 5.7. The transmission loss estimates show at least a 10-dB variation in received source levels as the ship passes the mooring. Variability due to sea surface state is estimated to be at least 5 dB with the IQR of the model data.
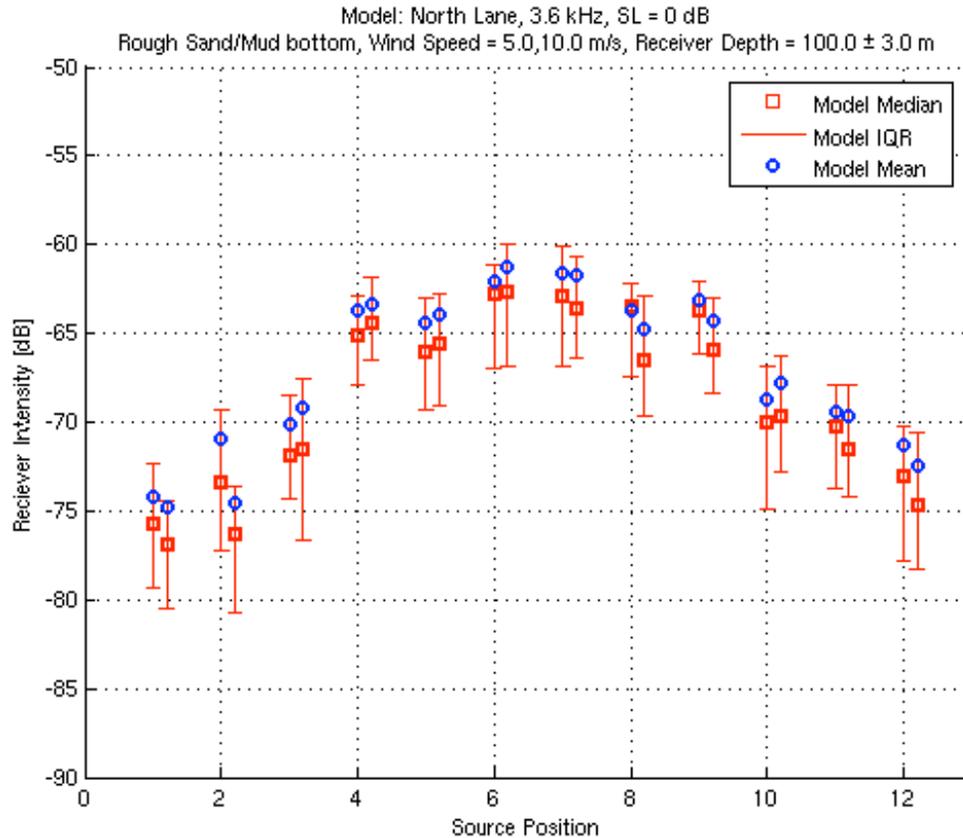
Figure 5.8 Model results for transmission loss associated with shipping lane traffic (as shown in Figures 5.7). The mean and standard deviation of the model results are obtained by Monte-Carlo simulations with 20 realizations of a random sea surface and bottom roughness.

5.5.   Analysis: Comparison with Lloyd mirror effect

Basic theoretical acoustic modeling considerations provide a 1) check to see if the results presented in the previous section are reasonable, and 2) method to extrapolate the results to frequencies other than 3.6 kHz.

The sound speed in the waters of Haro Strait is nearly constant (Section 2.3) and the surface acts as a reflector while the bottom acts as an absorber of acoustic energy, at least to first order; the acoustic propagation problem in the Haro Strait is straight-forward. For any given acoustic point source (e.g., from cavitation due a ship's rotating propeller) at a depth z_s, a hydrophone at a horizontal distance r away from the ship, and at a depth z_r, the sound field is determined by the interference of two arrivals. The first arrival is the direct

arrival, which travels along the straight line path connecting the acoustic source and receiver. The second arrival has traveled along two straight lines, the first from the acoustic source to the sea surface, and the second from the sea surface to the receiver. Because the surface acts like a mirror for acoustic energy (at least when the roughness horizontal correlation length is small compared to the acoustic wavelength), there is a unique position on the surface for the reflected arrival that corresponds to the receiver position. This situation is very common and fundamental in acoustic propagation in the ocean, and the distinctive sound field pattern it yields has been named the Lloyd mirror effect.

Assuming all acoustic energy interacting with the bottom is completely absorbed, the expression for transmission loss for this idealized situation is given by

$$TL = 10\log\left[\frac{4}{r^2 + z_r^2}\sin^2\left(\frac{kz_s z_r}{\sqrt{r^2 + z_r^2}}\right)\right],$$ [5.2]

where the acoustic wave number is $k=2\pi/\lambda$, with λ being the acoustic wavelength. With all distances in the above expression given in meters, the acoustic wave number has units of inverse meters. For the acoustic frequency used here, 3.6 kHz, the wavelength is approximately 0.41 m. Using this information, Eq. 5.2 can be used to construct the transmission loss field plot (Figure 5.9). Notice the similarities of Figure 5.9 and the upper panel of Figure 5.1, which is a transmission loss field plot assuming a flat surface and deterministic bottom (i.e., no bottom roughness). For short ranges of 1 km or less, the PE simulation reveals identifiable Lloyd mirror 'beams' observed at all ranges in Figure 5.9. Beyond about 1 km, the simple pattern of Figure 5.9 breaks down due to bottom interaction. For very short ranges, sound energy penetrates into the bottom at relatively steep angles with respect to the horizontal and is absorbed. Acoustic energy less steep reflects off the bottom. The angle with a cosine that is the ratio of the sound speed in the water to the sound speed at the top of the sediment at the water–sediment interface defines a critical angle whereby all acoustic energy that interacts with the bottom at angles less than this will be perfectly reflected. From the two representative bottom types used in this study (Table 5.1), the critical angles are determined to be 17 degrees for the sand/mud bottom, and 38 degrees for the rock/sand bottom. Going back to Figure 5.1, we observe that reflections from the bottom at about 500 m range, where the bottom depth is about 180 m. Not accounting for the bottom slope, the smallest angle at which acoustic energy interacting with the bottom reflects is at $\tan^{-1}\frac{180}{500} = 19$ degrees, which is in good agreement with the sand/mud bottom critical angle of 17 degrees.

Thus we expect that at about 1 km and beyond, more than two arrivals interfere with and contribute to a given receiver range and depth. If the sediment thickness is significantly greater than the acoustic wavelength, this effect is independent of acoustic frequency. In this case, it is easy to extrapolate to both higher and lower frequencies of propagation. The number of beams in the Lloyd mirror pattern increases with frequency, however, as will the absorption in the water volume, but this will modify the transmission loss in a slight and predictable manner.
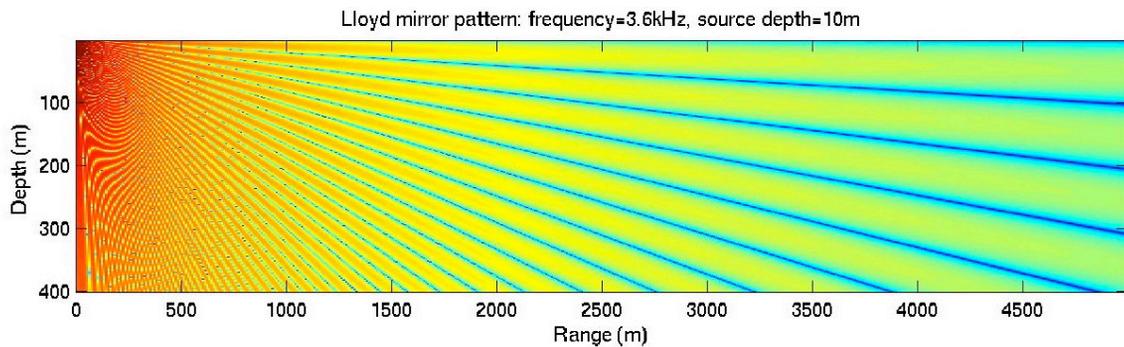

Figure 5.9. Transmission loss due to propagation in an idealized environment composed of a constant sound speed (1482 m/s), flat surface (0 m/s wind speed), and perfectly absorbing bottom, using an acoustic frequency of 3.6 kHz. An 80-dB dynamic range is shown, dark red indicating highest sound intensity, and dark blue the lowest.

Where the sediment thickness is smaller than the acoustic wavelength, extrapolating to lower frequencies becomes more problematic because the lower frequency acoustic energy will in effect not 'feel' the sediment layer, and the critical angle will be determined by the underlying substrate material, which could have a much different sound speed value. Thus, the critical angle for the lower frequency sound would then be different than at the higher frequencies. This shows a sensitivity of model output to one of the most fundamental inputs in the acoustic model, the geo-acoustic properties of the bottom. With the very limited information on the geo-acoustics of Haro Strait, it would be difficult to perform model–data comparisons at frequencies lower than 100 Hz.

Both roughness of the surface and roughness of the sea bottom cause the sound to scatter, so that instead of reflecting the sound at the same angle at which it impinged the surface or bottom, the sound emanates from the surface or bottom in all directions. The amount of sound that reflects at the same angle at which it impinged the surface or bottom depends on the surface/bottom roughness compared to the acoustic wavelength. A convenient way to express this is through the Rayleigh parameter:

$$R = \frac{2\pi}{\lambda} H \sin \vartheta. \qquad\qquad [5.3]$$

Here H is the RMS height of either the surface or bottom, ϑ is the angle at which the acoustic wave interacts with the surface, and λ is the acoustic wavelength. The amount of acoustic energy that remains coherent, or in the direction it would have gone if it had interacted with a flat surface (or flat bottom at angles less than the critical angle described above), is given approximately as $\exp(-R^2)$. As an example, using the RMS height for the bottom roughness H=0.4 m (Section 5.2.3), λ=0.5m (corresponding closely with the acoustic frequency of 3.2 KHz), and a nominal angle of ϑ=15 degrees, one finds that the Rayleigh parameter R is about 1.3, so that only 20% of the acoustic energy that interacts with the bottom at less than critical angles remains coherent. This loss of coherence is observed as a 'smearing' of the beams that have interacted with both the surface and bottom (Figure 5.3, for example). Extrapolating to lower frequencies yields a proportionally smaller Rayleigh parameter, and the exponential dependence indicates that the acoustic energy will remain coherent for much greater ranges, even for very rough surfaces, corresponding to high wind conditions.

A final issue of importance relating to this Lloyd mirror problem is worth noting. For sufficiently long ranges ($r \gg z_s$), the expression in Eq. 5.2 simplifies to $TL \cong 40 \log r$, which is twice the amount of transmission loss that would occur if there were no surface (spherical spreading), and this overall destructive interference effect is independent of the acoustic frequency. This can provide an important check with lower frequency data, where roughness is negligible.

6.   Recommendations

6.1.   Measurement strategies

It is our recommendation that acoustic modeling in Haro Strait is best used as a complement to field measurements, as the environment is far too complex, and the geo-acoustic parameters of the area are not characterized well enough to rely on modeling alone. However, to develop further confidence in the models and to enable them as a tool for prediction, several controlled measurements should be done, which to the best of our knowledge have not been performed. These experiments should be designed to measure quantities that can be compared directly with modeling results and specifically designed to investigate propagation from the shipping channel.

Several cost effective acoustic experiments are appropriate at this time. In particular, focusing on shipping noise estimates, several measurements would be useful:

1. *Direct measurements of transmission loss using a known source in the shipping channel*. These measurements would address commercial shipping traffic noise and be related directly to the modeling approach described here. Measurements could be made using a calibrated source located in the shipping channel and calibrated receivers at several locations of interest outside the shipping channel, such as along the coast of San Juan Island. Such measurements should include:
    a. Narrow frequency band measurements (long tones) to better compare data with existing propagation models. This can be done cost effectively using a recording instrument like the PALs and a hand held source deployed over the side of a small boat. The source levels would be low (comparable to ship source levels) to avoid animal disturbance. Measurement data would be directly comparable to simulations of transmission loss, providing insight into the validity and accuracy of a PE modeling approach.
    b. Broadband sources (short pulses) to address the issue of reverberation and backscatter from the channel walls. In direct comparison with the above measures this would address the relative importance of reverberation in the area. The difficulty with these measurements, however, is that the source levels for the short pulses must be relatively high to make reliable measurements, compared to the longer tones. So care must be taken to avoid animal disturbance.

2. *Longer term recordings of shipping noise*. These types of measurements could be used to investigate:
    a. Seasonal variation in the background noise levels that could be correlated with the changing oceanographic and weather conditions

b. Regional variation with receivers at several locations in the strait to sample the wide range of geographic conditions

c. Correlation of seasonal and regional measures of background sound levels with records of killer whale locations over time

Each of these measurements would require a cost effective acoustic receiver. To measure background sounds levels, averaged spectral data is sufficient and reduces the data storage requirements. Time series data is not necessary unless transient signals (i.e., whale vocalizations) are also desired. In the case of time series data, the receivers would require either a cable to shore or radio (wifi for short distance) connection to land. For time series data recording over long periods, data processing and storage requirements are significant and should be addressed up front. Given these limitation, it is recommended that spectral type recording (requiring much less data storage and processing) be used.

3. *Direct measurements of broadband source levels of large ships and tugs in the main shipping traffic lanes.* This is necessary because no data exist on ship source levels. Therefore, the model-based inversions made from a distance are not validated. A simple way to do this is to put a mooring in the shipping channel (using a PAL or a similar instrument) to record ship signals as they pass overhead. With this geometry the ships' sound source levels are measured at very short ranges and propagation effects are reduced significantly, allowing for good estimates of the true source levels of the ships in situ. The VTOSS database could then be used to compile statistics on ship noise with ship type, speed, and orientation. With good information on the true source levels of ships, model results and data from remote sites (not in the ship lanes) can then be used to address the sound exposure levels over larger areas and at different times of the year. Combined with models and other data, this would also provide a baseline measurement of sound levels in the strait that could be used to address long-term trends and impact.

Implicit in these recommendations is the appreciation for the practical value of developing a modeling capability. This comes in part from experience, as measurements are generally much easier to make than they are to understand. Acoustic measurements always require thoughtful interpretation, which usually requires a propagation model, unless the recordings are made at very short ranges or in very simple environments. With confidence in a modeling strategy, models can then be used to extrapolate data to other regions of the strait where measurements are not available, and to predict sound levels for potential scenarios such as Naval operations or increased commercial shipping traffic.

6.2.   Estimation of total shipping noise

Total background sound levels can always be measured directly with in-situ hydrophones. But to cover the relatively large area of the Haro Strait, many sensors would be required. In the final analysis, it is also desirable to know where the sound is coming from, as opposed to combined measurements of all the sound sources in an area. For example, a relevant question in the strait may be: what is the total background noise level due to commercial shipping vs. pleasure boats or commercial whale watching boats?

The combination of propagation modeling of the shipping lanes, selective in-situ measurements, and the VTOSS database can be used to address noise partitioning and provide an estimate of *total* shipping noise within the region at different times of the year. In principle, the basic method is straight forward: use the VTOSS database to identify the times and ranges of ships that pass within a specified area and then use the propagation model to estimate the sound levels at a specific location or set of locations.

The estimates of ship source levels can be handled in two ways. First, one could rely completely on assumptions about ship source levels, or as mentioned above, use direct measurements of ship sound source levels to validate model/data inversions for a set of representative ships. Alternatively, one could use long-term recordings from a single location (such as done in this report using the PAL data) to invert for ship source levels. This can done using the VTOSS ship tracks and times to identify individual signatures in the PAL data (Section 4.3). Then the measured data can be fit to the transmission loss curve for the average shipping lane, providing source levels of the ships (Section 5.4.1).

Because the majority of large ships travel within the narrow shipping lane, numerical simulations for the average ship lane track should be sufficient, as opposed to performing numerical simulations for each individual ship track. Errors associated with the track deviation within the lane should be minimal, as variability due to surface roughness and bottom type uncertainty are on the order of 5 dB and likely as large as the deviation due to source position errors on the order of 100 m. Problems will arise when there is more than one ship contributing to the sound recorded at a specific time. However, by looking at enough data over time there will likely be enough times when individual ship signatures can be identified and a representative picture of ship traffic source levels should be able to be compiled. Alternatively, one could assume that the sound source add incoherently.

6.3.   Further VTOSS analysis

The VTOSS database of ship traffic is itself a valuable database for analysis, and future studies could involve:

1. Developing an archiving of VTOSS data to compile statistics of shipping traffic in the region.
2. The correlation of shipping data (track density, ship type, speed, etc.) with data on animal locations and movements.
3. Integration of other databases on the acoustic characteristics of ships with the VTOSS data to provide a merged database of ship acoustic source level and position. For example, the combined information on engine type, prop length, draft, hull length, etc., and information on ship speed and orientation (as provided by VTOSS) can be used to better predict source level. Classifying or estimating ship source levels from ship characteristics is a longer-term goal, whereas direct measurements (as recommended above in Section 6.1.3) can be used in the shorter term and as a way to test predictions. Although this would not be a trivial task, one could potentially use this information to model the source level and source directivity of most of the commercial ships passing through Haro Strait. A paper by Wales et al. discusses recent advances in ship source modeling.[16]

6.4.   Reverberation modeling

Because the acoustic mooring was situated in deep water, and the dominant sound sources were ships in the Haro Strait shipping lanes, backscattering off the steep western shore of San Juan Island was not deemed significant, at least as far as what would be measured on the PAL. However, it is known that the southern resident killer whales feed very close to shore along the west coast of San Juan Island. The slope is very steep in this region, and strong upslope enhancement is anticipated, as well as horizontal refraction from bottom interaction.[17] Although this problem falls under the category of reverberation, the dominant acoustic signal would be from a focusing effect caused by sound energy propagating at successively steeper angles as it interacts with the up-sloping bottom.

It would be very useful to predict this enhancement of the sound intensity. This could be done with a three-dimensional ray model. To first order, one could assume a flat surface,

---

[16] Wales, S.C., and R.M. Heitmeyer, 2002. "An ensemble source spectra model for merchant ship-radiated noise," *J. Acoust. Soc. Am.*, 111, 1211–1231.

[17] Harrison, C.H., 1977. "Three-dimensional ray paths in basins, troughs, and near seamounts by use of ray invariants," *J. Acoust. Soc. Am.*, 62, 1382–1388.

use an iso-velocity sound speed field, and assume perfectly reflecting rock for the geo-acoustic properties of the near shore bottom. One could then map out the potential regions of acoustic focusing or 'hot spots' that would occur at particular locations of ship sources.

REPORT DOCUMENTATION PAGE

1. AGENCY USE ONLY *(Leave blank)*	2. REPORT DATE July 2006	3. REPORT TYPE AND DATES COVERED Technical Memorandum

4. TITLE AND SUBTITLE

Acoustic Environment of Haro Strait:
Preliminary Propagation Modeling and Data Analysis

5. FUNDING NUMBERS

NOAA AB133F-04-SE-1218

6. AUTHOR(S)

Christopher D. Jones and Michael A. Wolfson

7. PERFORMING ORGANIZATION NAME(S) AND ADDRESS(ES)

Applied Physics Laboratory
University of Washington
1013 NE 40th Street
Seattle, WA 98105-6698

8. PERFORMING ORGANIZATION REPORT NUMBER

APL-UW TM 3-06

9. SPONSORING / MONITORING AGENCY NAME(S) AND ADDRESS(ES)

Randall Brown (Contracting Officer)
NOAA
Western Regional Acquisition Divisio
7600 Sand Point Way NE/WC
Seattle, WA 98115-6349

10. SPONSORING / MONITORING AGENCY REPORT NUMBER

11. SUPPLEMENTARY NOTES

12a. DISTRIBUTION / AVAILABILITY STATEMENT

Proposed: Approved for public release; distribution is unlimited.

12b. DISTRIBUTION CODE

13. ABSTRACT *(Maximum 200 words)*

Field measurements and acoustic propagation modeling for the frequency range 1–10 kHz are combined to analyze the acoustic environment of Haro Strait of Puget Sound, home to the southern resident killer whales. Haro Strait is a highly variable acoustic environment with active commercial shipping, whale watching, and Naval activity. Southern resident killer whales are of unique public concern in this area because of increasing anthropogenic noise levels that may interfere with the animal's foraging strategies and behavior. Predictive acoustic modeling in combination with field measurements can be used as a tool for understanding the mechanisms of impact and assessment of the risk, providing a quantitative evaluation of sound source levels in the context of complicated acoustic environments, changing background sound levels, and emerging management issues. Of principle concern here is background sound levels created by commercial shipping traffic or other persistent sound sources that propagate from the main shipping channel. The scope of the modeling effort encompasses numerical modeling of transmission loss and propagation at ranges of less than 10 km. Preliminary modeling results are analyzed and compared with recordings of ship noise collected in the spring/summer of 2004.

14. SUBJECT TERMS

Haro Strait, Puget Sound, acoustic environment, shallow water, acoustic model, southern resident killer whales, shipping noise

15. NUMBER OF PAGES

51

16. PRICE CODE

17. SECURITY CLASSIFICATION OF REPORT Unclassified	18. SECURITY CLASSIFICATION OF THIS PAGE Unclassified	19. SECURITY CLASSIFICATION OF ABSTRACT Unclassified	20. LIMITATION OF ABSTRACT SAR